# Sea surface temperature reconstruction in the Pacific Ocean using multi-elemental proxy in *Porites* and *Diploastrea* corals: application to Palau Archipelago

Marine Canesi[1,2,3 *], Eric Douville[1], Paolo Montagna[4], Louise Bordier[1], Sandrine Caquineau[5], Edwige Pons-Branchu[1], Guillaume Iwankow[6], Jarosław Stolarski[7], Denis Allemand[2,3], Serge Planes[6], Clémentine Moulin[8], Fabien Lombard[9], Guillaume Bourdin[9,10], Romain Troublé[8], Sylvain Agostini[11], Bernard Banaigs[6], Emilie Boissin[6], Emmanuel Boss[10], Chris Bowler[12], Colomban de Vargas[13], Michel Flores[14], Didier Forcioli[3,15,16], Paola Furla[3,15,16], Eric Gilson[3,15,16,17], Pierre E. Galand[18], Stéphane Pesant[19], Shinichi Sunagawa[20], Olivier Thomas[21], Rebecca Vega Thurber[22], Christian R. Voolstra[23], Patrick Wincker[24], Didier Zoccola[2,3], Stéphanie Reynaud[2,3]

[1] Laboratoire des Sciences du Climat et de l'Environnement, LSCE/IPSL, CEA-CNRS-UVSQ, Université Paris-Saclay, 911 91 Gif-sur-Yvette, France

[2] Centre Scientifique de Monaco, 8 Quai Antoine Ier, 98000 Monaco, Principality of Monaco, Monaco

[3] LIA ROPSE, Laboratoire International Associé Université Côte d'Azur - Centre Scientifique de Monaco, Monaco

[4] Istituto di Scienze Polari (ISP), Consiglio Nazionale delle Ricerche (CNR), Via Gobetti 101, 40129 Bologna, Italy

[5] LOCEAN Laboratory, IRD-CNRS-Sorbonne Université-MNHN, IRD France-Nord, 93143 Bondy cedex, France

[6] Laboratoire d'Excellence "CORAIL," PSL Research University: EPHE-UPVD-CNRS, USR 3278 CRIOBE, Université de Perpignan, 66100 Perpignan, France

[7] Institute of Paleobiology, Polish Academy of Sciences, PL-00-818 Warsaw, Poland

[8] Fondation Tara Océan, Base Tara, 75012 Paris, France

[9] Sorbonne Université, Institut de la Mer de Villefranche sur mer, Laboratoire d'Océanographie de Villefranche, 06230 Villefranche-sur-Mer, France.

[10] School of Marine Sciences, University of Maine, Orono, Maine, United States of America.

[11] Shimoda Marine Research Center, University of Tsukuba, Shimoda, Shizuoka, Japan

[12] Institut de Biologie de l'Ecole Normale Supérieure (IBENS), Ecole normale supérieure, CNRS, INSERM, Université PSL, 75005 Paris, France

[13] Sorbonne Université, CNRS, Station Biologique de Roscoff, AD2M, UMR 7144, ECOMAP, 29680 Roscoff, France

[14] Weizmann Institute of Science, Department of Earth and Planetary Sciences, 76100 Rehovot, Israel

[15] Université Côte d'Azur, CNRS, INSERM, Institute for Research on Cancer and Aging, Nice (IRCAN), Nice, France

[16] Université Côte d'Azur, Institut Fédératif de Recherche - Ressources Marines (IFR MARRES), Nice, France

[17] Department of Medical Genetics, CHU Nice, France

[18] Sorbonne Université, CNRS, Laboratoire d'Ecogéochimie des Environnements Benthiques (LECOB), Observatoire Océanologique de Banyuls, 66650 Banyuls sur mer, France

[19] PANGEA, Data Publisher for Earth and Environment Science, Bremen, Germany

[20] Department of Biology, Institute of Microbiology and Swiss Institute of Bioinformatics, ETH Zürich, CH-8093 Zürich, Switzerland

[21] Marine Biodiscovery Laboratory, School of Chemistry and Ryan Institute, National University of Ireland, Galway, Ireland

[22] Oregon State University, Department of Microbiology, 220 Nash Hall, 97331Corvallis OR, USA

[23] Department of Biology, University of Konstanz, 78457 Konstanz, Germany

[24] Génomique Métabolique, Genoscope, Institut François Jacob, CEA, CNRS, Univ Evry, Université Paris-Saclay, 91057 Evry, France

*** Corresponding author** at: Laboratoire des Sciences du Climat et de l'Environnement (LSCE), Ormedes Merisiers, 91191 Gif-sur-Yvette, France.

*E-mail address*: marine.canesi@gmail.com (Marine Canesi).

## Abstract

Massive reef-building *Porites* corals are commonly studied to obtain long-term reconstructions of past sea surface temperature (SST) using temperature-sensitive elemental proxies, such as Sr/Ca or Li/Mg ratios. Most recently, a multi-proxy approach combining these two ratios (e.g. D'Olivo et al., 2018) and the Sr-U method (DeCarlo et al., 2016) have proved to be more robust to reconstruct paleo-temperatures. To date, no study has been carried out on the application of these new approaches on the *Diploastrea heliopora* coral, another massive reef-building genus that can potentially provide longer temperature records. Moreover, only a few studies have assessed coral SST calibrations at the scale of the Indo-Pacific basin and compared SST reconstructions obtained from two massive coral genera from the same site.

In this study, we investigated the elemental composition of the topmost portion of 34 modern tropical *Porites* and 6 *Diploastrea* colonies collected during the Tara Pacific expedition (2016 - 2018) from various hydrological contexts in the Pacific Ocean. We derived and discussed annual Sr/Ca, Li/Mg, combined Sr/Ca-Li/Mg and Sr/Ca-Li/Ca-Mg/Ca and Sr-U *vs*. SST calibrations as well as potential intra-colonial and genus specific effects and evaluated the use of these basin-wide calibration equations. Overall, multi-ratio and multi-genera SST calibrations perform better than single-ratio calibrations and seem to improve temperature reconstructions.

These new SST calibrations were applied to two colonies of *Porites* and *Diploastrea* collected from the same site in the North-West of the Palau archipelago located in the western Pacific Ocean to evaluate the applicability of universal calibrations based on different proxies and their combination. Coral-based SST records spanning the last 141 years show decadal changes and recent warming episodes that are related to major El Niño Southern Oscillation events. However, differences in reconstruction remain between both genera in the long-term trends, amplitudes, and absolute temperatures, depending on which genus or temperature proxy is considered.



## Keywords

Massive tropical corals, Sea Surface Temperature, Calibrations, Elemental proxies and SST reconstructions, Pacific Ocean

## 1. Introduction

Since the beginning of the industrial era, the $CO_2$ concentration in the atmosphere has increased from 280 to more than 400 ppm (Friedlingstein et al., 2022). Model projections suggest that the rise in atmospheric $CO_2$ concentration will likely contribute to a global surface temperature increase of 1.0 to 5.7°C (compared to 1850-1900) by the end of the 21$^{st}$ century, depending on the greenhouse gas (GHGs) emission scenario considered (IPCC, 2021). The surface ocean absorbs about 90% of the excess heat attributed to GHGs and approximately one-third of the anthropogenic $CO_2$ emissions (Stocker et al., 2013), which increases the temperature and acidity of the ocean and, consequently, negatively impacts marine ecosystems over the long term. Calcifying organisms, such as tropical corals, are among the most threatened organisms by these global changes (Hoegh-Guldberg, 1999; Kleypas et al., 1999; Hoegh-Guldberg et al., 2007; Kroeker et al., 2013; Dutra et al., 2021). In particular, seawater warming can alter the calcification processes and increase the frequency of bleaching events (Hughes et al., 2017). Assessing long-term coral responses to global warming or episodic high-temperature events is crucial to better understand their adaptability and resilience to climate changes over time. One way to evaluate those potential impacts is to reconstruct past environmental variations, such as Sea Surface Temperature (SST) or pH, using the growth parameters or the geochemistry of reef-building scleractinian coral skeletons (e.g. Gagan et al., 2000; Lough, 2010).

The skeleton of the genus *Porites* grows at approximately 1 cm per year on average (from a few millimeters to up to 3 cm per year) (Lough et al., 2008; Goodkin et al., 2011) and typically shows well-defined seasonal density bands. This reef-building coral is commonly used in paleoceanography to reconstruct decadal to centennial-scale records of key environmental parameters at annual to seasonal resolution in the tropical regions and study the ocean-atmosphere interaction processes (e.g. Tangri et al., 2018). The *Diploastrea* genus has been investigated as an archive for paleo SST and pH reconstructions (Watanabe et al., 2003; Damassa et al., 2006; Ramos et al., 2017; Wu et al., 2018). *Diploastrea* has a slower (few millimeters per year) growth rate than *Porites*, hence it can provide longer records for similar core length (e.g. Bagnato et al., 2004), spanning more than 700 years (Burr et al., 1998; Corrège et al., 2004). However, the larger and more complex skeletal (micro-) structures of *Diploastrea* make the SST reconstructions more challenging as previously shown for oxygen isotopes (Watanabe et al., 2003; Bagnato et al., 2004; Damassa et al., 2006). *Diploastrea*'s geographic occurrence covers much of the Indo-Pacific Warm Pool, the western Indian Ocean, and the Great Barrier Reef (Veron, 2000; DeVantier and Turak, 2017), allowing studies on climate variability and its impact in regions with extensive coral reefs, as well as on the hydrodynamical connections between the Indian and western Pacific Ocean.

Reconstructions of paleo-SST from coral samples have commonly relied on the ratios of isotopes and elements such as $\delta^{18}O$, Sr/Ca, and to a lesser extend U/Ca and Mg/Ca (e.g. Weber and Woodhead,

1972; Beck et al., 1992; Min et al., 1995; Mitsuguchi et al., 1996; Wei et al., 2000; Fallon et al., 2003; Montagna et al., 2007). Among these geochemical proxies, the most commonly used in tropical corals is the Sr/Ca ratio (Beck et al., 1992; Quinn and Sampson, 2002; DeLong et al., 2007; Pfeiffer et al., 2009; Zinke et al., 2014). However, biases on SST estimates from coral Sr/Ca have been reported due to the activity of the coral-associated algal symbionts (Cohen et al., 2002), skeletal heterogeneity (e.g. Cohen et al., 2001), diagenetic modifications (e.g. Hendy et al., 2007) and biomineralization processes (Corrège, 2006; DeLong et al., 2013). The U/Ca ratio in corals is a complex geochemical proxy, being influenced by multiple environmental factors such as temperature, salinity, meteoric precipitation, pH, carbonate ion concentration and saturation state (Shen and Dunbar, 1995; Wei et al., 2000; Inoue et al., 2011; Wu et al., 2021).

There is growing evidence that physiological processes and/or growth-related kinetic effects, commonly known as "vital effects", can influence Sr/Ca, as well as Mg/Ca, U/Ca, and $\delta^{18}O$ in shallow and deep-water corals and consequently the temperature reconstructions (e.g. Finch and Allison, 2008; Meibom et al., 2004; Montagna et al., 2005; Sinclair and Risk, 2006; López-Correa et al., 2010; Montagna et al., 2014; Cuny-Guirriec et al., 2019), especially the varying growth rates at different spatial scales, from the colony to the coral microstructures (D'Olivo et al., 2018). The extent to which these biological and kinetic factors can bias past SST reconstructions is still poorly known and is an ongoing research topic in coral geochemistry (e.g. Flannery et al., 2018; Cuny-Guirriec et al., 2019). In addition, early diagenesis, secondary aragonite, calcite precipitation, and/or the presence of organic matter may impact the accuracy and precision of SST reconstructions, and such effects need to be precisely evaluated (Allison et al., 2007; Lazareth et al., 2016; Cuny-Guirriec et al., 2019).

Alternative approaches to reconstruct paleo-SST include the use of a Rayleigh-based, multi-element approach (Gaetani et al., 2011; Sinclair, 2015), coral core replications (DeLong et al., 2013), and growth-dependent calibrations of Sr/Ca (Goodkin et al., 2007; Saenger et al., 2008). Recently, the development of new paleo-thermometers such as Li/Ca (Marriott et al., 2004; Hathorne et al., 2013), Li/Mg (Case et al., 2010; Montagna et al., 2014; Marchitto et al., 2018; Cuny-Guirriec et al., 2019) and Sr-U (DeCarlo et al., 2016) contributed to improve the reliability of the coral-based SST reconstructions. Several trace elements, including Li, Mg, U and Sr, might be affected by the Rayleigh fractionation or by active and passive transport of ions into the calcifying fluid (e.g., via diffusion, paracellular pathways, and $Ca^{2+}$-ATPase pump) during their incorporation into the coral skeleton (Gaetani and Cohen, 2006; Gagnon et al., 2007; Gaetani et al., 2011; Ram and Erez, 2021; 2023). The normalization of Li to Mg (or Mg to Li) is thought to eliminate the influence of these processes, such that temperature remains the main environmental parameter controlling the coral Li/Mg (or Mg/Li) ratio (Case et al., 2010; Montagna et al., 2014; Marchitto et al., 2018). Unlike Sr/Ca, the Li/Mg-SST calibration can be extended to a large range of zooxanthellate and azooxanthellate coral species covering a wide temperature range (from sub-freezing to tropical temperatures) (Montagna et al., 2014; Cuny-Guirriec et al., 2019). However, the uncertainty of the Li/Mg exponential equation is

rather high (± 2.6°C at 25°C) for tropical corals (e.g. *Siderastrea*, *Porites,* or *Diploastrea*) compared to cold-water corals (± 0.9°C at 1 °C), due to the asymptotic behavior of the equation at higher temperatures (Cuny-Guirriec et al., 2019).

The Sr-U thermometry was developed by DeCarlo et al. (2016) and it is based on the combined measurements of Sr/Ca and U/Ca that minimize "vital effects". In particular, U/Ca is used to correct for effects related to Rayleigh fractionation on Sr/Ca, which improves the accuracy of SST reconstructions.

Finally, few studies have developed and applied a multi-proxy approach, which combines different temperature-sensitive elements (e.g. Li, Mg, Sr, U) into a multi-regression model that reduces the temperature uncertainty (Quinn and Sampson, 2002; Solow and Huppert, 2004; Fowell et al., 2016; D'Olivo et al., 2018; Cuny-Guirriec et al., 2019; Zinke et al., 2019; Wu et al., 2021), yet further studies are required to properly evaluate their caveats and constraints.

The present study reports the Sr/Ca, Li/Ca, Mg/Ca, U/Ca, and Li/Mg ratios obtained from the topmost portion of 40 modern colonies of *Porites* and *Diploastrea* collected from various locations in the Pacific Ocean with the aim to re-evaluate single and multi-ratio universal SST calibrations. The main purpose of applying universal calibrations is to generate SST data when direct calibration is not possible, such as with fossil coral samples. These calibrations were then applied to two *Porites* and *Diploastrea* long-cores retrieved from the northern part of the Koror Island (Palau, western Pacific Ocean) to 1) reconstruct SST changes over the last century, 2) evaluate the genus-specific discrepancies, and 3) compare annual and decadal SST records based on different proxies and calibration equations. It is worth mentioning that the present study does not evaluate the fidelity of the different proxies to record SST but rather it examines the applicability of universal calibrations based on different proxies and their combinations. The different sources of uncertainties in the SST proxies and calibration equations were also investigated, which includes the impact of the growth parameters in modifying the geochemical signals, the intra-colonial or genus effects, and the different strategies of coral sub-sampling (e.g., bulk sampling or selected microstructures).

## 2. Material and methods

### 2.1. Sampling locations of coral cores

Forty coral cores were collected from massive *Porites* and *Diploastrea* colonies during the Tara Pacific expedition (Planes et al., 2019) between May 2016 and October 2018 from different sites in the Pacific Ocean (Fig. 1). *Porites* colonies were found in all atolls and islands visited during the expedition, whereas *Diploastrea* colonies were mainly encountered in the western Pacific Ocean. The cores (40 – 150 cm long) were collected from colonies living between 3 m (Moorea Island) and 20 m (Wallis Islands) depth using a hydraulic drill (Stanley®) with a 7-cm-diameter core barrel. They were rinsed with fresh water, air-dried, and stored for sclerochronological and geochemical analyses. The

mean annual seawater temperature at the sampling sites ranged from 22.4°C (Easter Island, Chile) to 29.8°C (Kimbe Island, Papua New Guinea).

Two long cores of *Porites* and *Diploastrea* were collected in January 2018 at site I26S1 in the north-western side of the Republic of Palau (7°17'N, 134°15'E) at 15 and 16 m water depth, respectively (Fig. 2). The archipelago of Palau is located in Micronesia in the western Indo-Pacific Warm Pool (IPWP), which is a key region for the global distribution of heat and moisture to the atmosphere (Wang and Mehta, 2008). The mean SST in Palau for the period 1982 – 2016 (28.78 ± 0.40°C, 1σ) was obtained from monthly data of the AVHRR-OISSTv2 dataset (Advanced Very High Resolution Reconstructed Optimum Interpolation Sea Surface Temperature version 2; Reynolds et al., 2007; Banzon et al., 2016). The annual temperatures ranged from 27.84 to 29.67 °C (ΔT ~ 1.8 °C) over the same period and increased at a rate of 0.23 ± 0.04 °C/decade. In 1998 and 2010, thermal-stress events occurred in Palau with temperatures 1 to 1.25 °C above the mean long-term value, relative to the period 1984 - 1993 (exclusive of 1991/1992), during La Niña episodes (Bruno et al., 2001; Colin, 2018). These warming events caused severe bleaching and mortality of corals, particularly in the north-western lagoon of Palau where the cores were collected (van Woesik et al., 2012; Colin, 2018).

## 2.2. Sclerochronology and coral age model

### 2.2.1. X-ray radiography and computed tomography

The X-ray radiography and 3D computed tomography allow visualizing the annual high- and low-density band couplets. These reflect the seasonal variations in skeletal density and are used to derive coral age models for paleoclimate reconstructions and to investigate coral growth variability over time (Knutson et al., 1972; Lough and Barnes, 1992; DeCarlo and Cohen, 2017). The 40 coral cores were scanned using a DISCOVERY CT750 high-definition computed tomography (CT) scanner at the DOSEO Platform, CEA-Paris-Saclay. The spatial x resolution of the scans is 0.625 mm while y and z resolutions range from 0.59 to 0.79 mm. 3D CT scans were processed using 3D Slicer® software (version 4.9.0) to visualize the 3D images. Linear extension rates ($mm \cdot yr^{-1}$) (upward linear growth) were obtained from each coral core by measuring the distance between successive low-density bands over the last 6 years of growth (2010-2016) (Fig. 3). Mean linear extension rate values (mean ±1σ) were calculated for each coral core by averaging linear extension measurements along 3 parallel transects.

The *Porites* and *Diploastrea* long cores from Palau were slabbed (8 mm) along the main growth axis with a circular saw at the *Atelier Saint-Jacques* (Saint-Rémy-lès-Chevreuse), rinsed with Milli-Q water, and dried at room temperate for 48 h. X-radiographs of both coral slabs were realized at the *Centre de radiographie* in Gif-sur-Yvette to visualize the maximal growth axis of both colonies and to optimize the sampling strategies.

### 2.2.2. U-Th Dating

The age model for the *Porites* and *Diploastrea* colonies from Palau obtained from the density banding was independently verified by $^{230}$Th/U dating at the *Laboratoire des Sciences du Climat et de l'Environnement* (LSCE, France). Three coral fragments were collected at the top, middle, and bottom portions of each core. The samples were crushed into small chunks, and ultra-sonicated in Milli-Q water. Each sample (~ 300 to 600 mg) was transferred to a Teflon beaker in which a known amount of $^{229}$Th, $^{233}$U, and $^{236}$U was previously added. Coral samples were dissolved in 3 - 4 mL of dilute HCl. After co-precipitation with FeOH, U and Th separation and purification were performed using UTEVA resin (Eichrom Technologies, USA) in nitric solution, following a procedure modified from Douville et al. (2010). U and Th isotopes were measured using a ThermoScientific Neptune$^{Plus}$ MC-ICP-MS fitted with a jet pump interface following the analytical protocol reported in Pons-Branchu et al. (2014). The $^{230}$Th/U ages were calculated from measured atomic ratios through iterative age estimation (Ludwig and Titterington, 1994), using the $^{230}$Th, $^{234}$U, and $^{238}$U decay constants of Cheng et al. (2013) and Jaffey et al. (1971). Our spike was calibrated against a Harwell Uraninite solution (HU-1) assumed to be at secular equilibrium. A correction was applied for the non-radiogenic (detrital) $^{230}$Th using a $^{230}$Th/$^{232}$Th activity ratio of 10 ± 3 (as in Wu et al., 2018).

## 2.3. Sampling strategy

From each of the forty 7-cm-diameter coral cores, a portion of ~ 1 g, corresponding to the last 6 years of growth (hereafter referred to as core-top), was collected along the major growth axis (Fig. 3) using a dental drill (Dremel®) with a 0.17 mm thick diamond-encrusted blade, finely crushed and thoroughly homogenized in an agate mortar. The uncertainty associated with the possible inclusion of skeleton from other years into coral samples (i.e., the effect from under-representing or over-representing a year) was quantified using the AVHRR-OISSTv2 dataset. For instance, adding either 6 warmer or colder months to the 6-year average (i.e., extending the 72 months by an additional 6 months) results in a temperature variation of up to 0.2°C across all the study locations (n = 40). This potential bias in coral sampling is lower than uncertainties from other sources (e.g., analytical errors and SST calibrations, see below) and supports our sampling strategy. In order to quantify the geochemical variability within core-top samples and assess intra-colonial reproducibility, the sub-sampling of the coral portion corresponding to the last 6 years of growth was triplicated in 3 different *Porites* cores (I5S4, I21S2c16, I22S2c2) living between ~ 22°C and ~ 30°C and a *Diploastrea* colony (I21S2c17), following the growth axis.

Different sub-sampling strategies were applied to the *Porites* and *Diploastrea* long-cores from Palau, according to their skeletal structures and linear growth rates. The sub-annual sampling of the *Porites* colony was conducted with an automatic 3-axes positioning system and a drill at 5 mm increments (Fig. 4). The *Diploastrea* colony was continuously sampled at 2.5 mm spatial resolution (sub-annual sampling) using a dental drill (Dremel®) with a 0.17 mm thick diamond-encrusted blade, following the

growth axis identified on the X-radiographs (Fig. 4). During the sampling, particular attention was paid to possible traces of secondary alteration of the coral skeleton. The assessment of possible diagenetic overprint was done by careful observations of the skeletal surfaces (detection of possible secondary aragonite/calcite crystals) and delicate etching of broken surfaces (detection of the possible presence of borings and their infillings with secondary minerals) using Scanning Electron Microscopy (SEM; Figs. 5, 6).

## 2.4. Geochemical analyses

### 2.4.1. Chemical treatment

The coral powders (~ 200 mg) were all treated in acid-cleaned vials following the oxidative cleaning protocol developed by Cuny-Guirriec et al. (2019) to remove the potential effects of organic contaminations on the trace element compositions. Samples were first sonicated in Milli-Q water for 30 s, cleaned with a mixture of 15% $H_2O_2$ buffered with 0.5 M $NH_4OH$, placed in a water bath at 60°C for 20 min, rinsed three times with Milli-Q water, and dried at 50°C overnight. Between each step, vials were centrifuged for 3 min and the supernatant discarded.

### 2.4.2. Quantitative multi-element analyses using ICP-QMS

Dried samples were dissolved in 1 N $HNO_3$ (Optima Fisher Ultra Trace Element Analysis, 67%) to obtain 100 ppm Ca solutions. Elemental (Li, B, Mg, Ca, Sr, U) concentrations were determined using a Quadrupole ICP-MS X-Series$^{II}$ at LSCE (Gif-sur-Yvette, France) using the protocol previously developed for carbonates (Bourdin et al., 2011; Montagna et al., 2014) and updated by Cuny-Guirriec et al. (2019). Blanks (0.5 N $HNO_3$) and the carbonate standards M1P-p (*Porites* sp. coral from Mayotte, in-house standard) and JCp-1 (*Porites*) (Okai et al., 2002) were routinely analyzed to bracket samples and monitor ICP-MS drift over time. Typical mean values and external reproducibility (2σ RSD) obtained from repeated measurements (n = 20) of the in-house carbonate standard M1P-p were: Li/Ca = 6.03 ± 0.15 μmol·mol$^{-1}$ (2.5 %), Mg/Ca = 4.37 ± 0.05 mmol·mol$^{-1}$ (1.1 %), Sr/Ca = 8.93 ± 0.06 mmol·mol$^{-1}$ (0.7 %), U/Ca = 1.09 ± 0.02 μmol·mol$^{-1}$ (1.8 %) and Li/Mg = 1.38 ± 0.02 mmol·mol$^{-1}$ (1.4 %). The mean values for JCp-1 were: Li/Ca = 6.23 ± 0.12 μmol·mol$^{-1}$ (1.9 %), Mg/Ca = 4.19 ± 0.03 mmol·mol$^{-1}$ (0.7 %), Sr/Ca = 8.86 ± 0.05 mmol·mol$^{-1}$ (0.6 %), U/Ca = 1.19 ± 0.02 μmol·mol$^{-1}$ (1.7 %) and Li/Mg = 1.49 ± 0.03 mmol·mol$^{-1}$ (2.0 %) (2σ RSD, n = 21), matching well mean values published by Hathorne et al. (2013) and Cuny-Guirriec et al. (2019).

## 2.5. Calcite characterization

Reliable SST reconstructions using coral Sr/Ca or Li/Mg depend on the preservation of the coral skeletal aragonite, which can be transformed into calcite due to early or post-mortem diagenetic processes, or on the presence of calcite traces associated with microborers or of primary origin (Lazareth et al., 2016; Cuny-Guirriec et al., 2019; Stolarski et al., 2011, 2021). The coral powders (~

100 mg) of the 40 core-tops and the recent and old parts of the *Porites* and *Diploastrea* colonies from Palau were analyzed using a Panalytical X'Pert Powder X-ray diffractometer (Ni-filtered CuKα radiation) operating at 40 kV and 40 mA with a counting time of $0.01°{\cdot}sec^{-1}$. Quantitative measurements of aragonite and calcite abundance were done through a calibration curve established for low calcite levels using ten in-house standards with known concentrations of aragonite and calcite (from 0.4 to 10 % of calcite). Each in-house standard was prepared and analyzed in triplicate. Areas of the (104) peak of calcite (3.03 Å) and (111) peak of aragonite (3.49 Å) were measured by peak fitting using the HighScore software (Panalytical, v.3.0). A linear regression was used for the calcite quantification:

$$\text{Calcite (\%)} = 27.1\ (A_c/A_a) - 0.1 \qquad R^2 = 0.99 \qquad \text{(Eq. A)}$$

where $A_c$ and $A_a$ are the areas under the calcite and aragonite peaks, respectively. A detection limit (DL) of 0.6 % of calcite and a mean error of 0.3 % ($2\sigma$) on the calcite percentage measurement were determined. XRD analyses were conducted on the same powdered samples analyzed for trace elements.

## 2.6. Instrumental temperature datasets

The mean seawater temperature at the sampling sites was obtained by averaging monthly SST data between January 2010 and December 2016 from the AVHRR-OISSTv2 dataset (Fig. 1). *In-situ* temperature records are available at a daily resolution only for 7 out of 34 coral sampling locations (Fiji, Wallis & Futuna, Palau, Samoa, Niue, Tahiti, and Papua New Guinea), mainly through the ReefTEMPS sensor network operating in the South, West and South-West Pacific (Cocquempot et al., 2019; Varillon et al., 2019), and the Water Temperature Catalogue in Palau (wtc.coralreefpalau.org). Maximum annual differences between AVHRR-OISSTv2 and *in-situ* SST data range from 0.03 °C (Samoa) to 0.67 °C (Tahiti). The largest differences result from the peculiar environment of some coral reefs, including the inner and outer reef or the internal lagoon, which is smaller than the spatial resolution covered by the AVHRR-OISSTv2 dataset (1/4°). For instance, the comparison between monthly *in-situ* and dataset temperatures at Ebiil Channel (Palau) shows mean monthly differences of 0.25 ± 0.46°C and 0.38 ± 0.42°C, for AVHRR-OISSTv2 and Extended Reconstructed Sea Surface Temperature (ERSSTv5) dataset (2°), respectively, with the largest offset being 0.95°C for both datasets. The difference is slightly larger when compared with ERSSTv5, which highlights the importance of using a high-resolution (1/4° *vs*. 2°) dataset.

The AVHRR-OISSTv2 dataset at 1/4° spatial resolution was used to derive the proxy-SST calibration equations. The mean SST value for each site was calculated as the average of the monthly SST from January 2010 to December 2016. This dataset was also used for comparison with the coral trace element records from Palau over the period 1982-2016. The *Diploastrea* long-term records were compared to the ERSSTv5 dataset, in the grid 7-9°N, 133-135°E, covering the period 1874-2016. SST anomalies were calculated relative to the mean of the period 1961-1990.

## 2.7. Calibrations and statistical analysis

Geochemical values of the core-tops corresponding to the period 2010-2016 were used to calculate linear regressions between SST and coral proxies. Single and multiple weighted robust regressions for Sr/Ca, Li/Ca, Mg/Ca, Li/Mg, and Sr-U *vs.* SST were obtained using iteratively reweighted least-squares with a bisquare weighting function of the statistical R Studio® software (version 1.1.463). Following the approach of Ross et al. (2019), the Sr-U value of each sub-sample was determined using the mean Sr/Ca and U/Ca ratios, based on equation 4 from DeCarlo et al. (2016):

$$Sr\text{-}U = Sr/Ca - (1.1107\ U/Ca)$$

Uncertainties in the temperature reconstruction for all calibration equations were calculated as the root-mean-square error (RMSE) (Bevington and Robinson, 1993). The analysis of the variance (one-way ANOVA test) was performed on the Palau time-series dataset to determine whether there were significant differences between the variances of the reconstructed and instrumental SST. The Mann-Kendall trend test was used to determine whether the time series has a significant monotonic upward or downward trend.

# 3. Results

## 3.1. Assessment of possible skeleton diagenetic alteration

The surfaces of *Porites* and *Diploastrea* skeletal parts were not covered with any secondary deposits (Figs. 5, 6) such as aragonite needle cements, brucite, or calcite which are easily detectable by distinct morphology, different from pristine biogenic material (e.g., Nothdurft and Webb, 2009: figs. 5, 6). In addition, the original pores between septa and columella were not infilled with any secondary deposits. Moreover, delicate etching of the skeleton showed that the microstructural organization is indistinguishable from skeletons considered pristine: the hollowed-up regions that represented Rapid Accretion Deposits (RAD's) were still composed of microcrystalline material, whereas the bulk of the skeleton consisted of Thickening Deposits ("fibers") often showing regular growth increments, typical of pristine skeletons of zooxanthellate corals (Stolarski, 2003; Frankowiak et al., 2016). Only exceptionally some traces of borings were detected that could be infilled by some secondary material (Figs. 5-D, 5-L, 6-F, 6-I).

The amount of calcite in the core-tops ranged from values below the detection limit (< 0.6 %) to 3.6 ± 0.3 % (2σ) for the *Porites* colony I15S1c10 from Guam, USA (Table 1). Two *Diploastrea* colonies from Papua New Guinea (I23S2D) and Taiwan (I28S3) contained traces of calcite (1 % and 1.4 %, respectively). Overall, the XRD analyses indicated that most of the samples contain a very small amount of calcite (mostly under the DL), confirming the preservation of skeletal aragonite of modern colonies collected during the Tara Pacific expedition.

The amount of calcite in the *Diploastrea* colony from Palau reached a maximum value of 2.8 ± 0.7 % in the sub-sample corresponding to the year 1874. Between 1895 and 2016, the amount of calcite was below the DL. The calcite percentage in the *Porites* long-core from Palau was systemically below the DL, except for the sub-sample corresponding to the year 2002, which showed a value slightly above the DL (0.8 %).

## 3.2. Coral core-tops

### 3.2.1. Linear extension rates

The linear extension rate of the studied core-tops varied among sites from 6.6 ± 0.6 $mm \cdot yr^{-1}$ in Ogasawara (Japan) to 16.7 ± 2.2 $mm \cdot yr^{-1}$ in Vangunu (Salomon) for *Porites*, and from 3.0 ± 0.7 $mm \cdot yr^{-1}$ in Noumea lagoon (New Caledonia) to 6.3 ± 1.4 $mm \cdot yr^{-1}$ in Green Island (Taiwan) for *Diploastrea* (Table 1). Extension rates measured in the 40 coral colonies were coherent with those reported in the literature for both genera, ranging from a few millimeters up to 30 $mm \cdot year^{-1}$ for *Porites* (Goodkin et al., 2011; Lough, 2008) and 2 to 5 $mm \cdot year^{-1}$ for *Diploastrea* (Bagnato et al., 2004; Corrège et al., 2004).

### 3.2.2. Coral elemental ratios

The mean molar ratios measured in the 34 *Porites* core-tops varied from 8.71 to 9.38 $mmol \cdot mol^{-1}$ for Sr/Ca, 5.37 to 7.21 $\mu mol \cdot mol^{-1}$ for Li/Ca, 3.55 to 5.29 $mmol \cdot mol^{-1}$ for Mg/Ca, 0.92 to 1.33 $\mu mol \cdot mol^{-1}$ for U/Ca, 1.18 to 2.00 $mmol \cdot mol^{-1}$ for Li/Mg and 7.55 to 7.92 for Sr-U (Table 1). The ratios for the 6 *Diploastrea* core-tops ranged from 8.76 to 9.04 $mmol \cdot mol^{-1}$ for Sr/Ca, 5.62 to 6.56 $\mu mol \cdot mol^{-1}$ for Li/Ca, 3.53 to 4.68 $mmol \cdot mol^{-1}$ for Mg/Ca, 0.96 to 1.13 $\mu mol \cdot mol^{-1}$ for U/Ca, 1.28 to 1.70 $mmol \cdot mol^{-1}$ for Li/Mg and 7.61 to 7.88 for Sr-U (Table 1).

**Table 1**

Coral sampling locations, elemental ratios, linear extension rates, and percentage of calcite for *Porites* and *Diploastrea* core-tops from the Pacific Ocean. The annual mean SST value for each site was sourced from the AVHRR-OISSTv2 dataset. Mean extension rates were calculated over the period 2010-2016. PNG = Papua New Guinea.

| Location | Core | Location | | Depth (m) | Sr/Ca mmol.mol$^{-1}$ | Li/Ca µmol.mol$^{-1}$ | Mg/Ca mmol.mol$^{-1}$ | Li/Mg mmol.mol$^{-1}$ | U/Ca µmol.mol$^{-1}$ | Sr-U | Gridded-SST Mean (°C) | Extension rate mm.yr$^{-1}$ | Calcite % |
|---|---|---|---|---|---|---|---|---|---|---|---|---|---|
| ***Porites* spp.** | | | | | | | | | | | | | |
| Coiba (Panama) | I2S3c21 | 07°12'N | 81°47'W | 8 | 9.01 | 5.85 | 4.26 | 1.37 | 1.13 | 7.75 | 28.59 | 9.80 | 1.0 |
| Anakena, Isla de Pascua (Chile) | I4S1 | 27°04'S | 109°19'W | 14 | 9.30 | 7.21 | 3.86 | 1.87 | 1.23 | 7.92 | 22.45 | 11.4 | < DL |
| Motu Taka Rua, Isla de Pascua (Chile) | I5S4 | 27°04'S | 109°19'W | 14 | 9.38 | 7.09 | 3.55 | 2,00 | 1.33 | 7.90 | 22.44 | 12.2 | < DL |
| Tekava, Gambier (French Polynesia) | I6S2 | 23°09'S | 134°50'W | 9 | 8.98 | 7.21 | 4.86 | 1.48 | 0.98 | 7.89 | 25.17 | 9.6 | < DL |
| Moorea (French Polynesia) | I7S1c1 | 17°28'S | 149°48'W | 3 | 8.91 | 6.31 | 4.66 | 1.36 | 1.09 | 7.69 | 27.77 | 11.6 | < DL |
| Moorea (French Polynesia) | I7S3c2 | 17°29'S | 149°45'W | 13 | 8.93 | 5.66 | 3.76 | 1.50 | 1.19 | 7.61 | 27.77 | 11.8 | < DL |
| Aitutaki, Cook (New Zeland) | I8S1c3 | 18°50'S | 159°48'W | 14 | 8.88 | 6.64 | 4.80 | 1.38 | 1.01 | 7.75 | 27.09 | 10.4 | < DL |
| S Niue (New Zeland) | I9S1c4 | 19°06'S | 169°54'W | 12 | 8.80 | 6.27 | 4.54 | 1.38 | 0.98 | 7.72 | 27,00 | 12.3 | < DL |
| W Niue (New Zeland) | I9S2c5 | 18°59'S | 169°54'W | 15 | 8.90 | 6.38 | 4.30 | 1.48 | 1.11 | 7.66 | 27.14 | 8.9 | < DL |
| Upolu (Samoa) | I10S0c6 | 13°50'S | 172°04'W | 9 | 8.83 | 5.76 | 4.19 | 1.38 | 1.03 | 7.69 | 28.81 | 10.9 | < DL |
| CSR 11, Wallis (France) | I11S1c7 | 13°18'S | 176°12'W | 20 | 8.84 | 6.85 | 5.29 | 1.29 | 0.92 | 7.81 | 28.97 | 8.8 | < DL |
| Abaiang (Kiribati) | I13S3c8 | 01°43'N | 172°58'E | 7 | 8.80 | 6.12 | 5.01 | 1.22 | 0.97 | 7.73 | 28.97 | 13.8 | < DL |
| Pisinun, Chuuk (Micronesia) | I14S2c9 | 07°08'N | 151°53'E | 8 | 8.76 | 5.73 | 4.49 | 1.27 | 1.03 | 7.62 | 29.23 | 10.9 | < DL |
| Guam (USA) | I15S1c10 | 13°14'N | 144°38'E | 9 | 8.76 | 5.83 | 4.89 | 1.19 | 0.94 | 7.71 | 28.92 | 9.9 | 3.6 |
| Ogasawara (Japan) | I16S2c11 | 27°05'N | 142°13'E | 5 | 9.23 | 6.75 | 3.75 | 1.80 | 1.31 | 7.77 | 24.30 | 6.6 | < DL |
| Sesoko, Okinawa (Japan) | I17 | 26°38'N | 127°51'E | 6 | 9.05 | 6.60 | 4.17 | 1.58 | 1.20 | 7.72 | 24.88 | 11.4 | < DL |
| NW Fiji | I18S1 | 17°22'S | 177°07'E | 7 | 8.84 | 6.07 | 4.47 | 1.36 | 1.03 | 7.69 | 28.03 | 12.0 | < DL |
| Heron, S GBR (Australia) | I19S1c13 | 23°26'S | 151°54'E | 7 | 9.09 | 6.98 | 4.17 | 1.67 | 1.18 | 7.77 | 24.43 | 8.9 | < DL |
| SW Cockatoo Reef, GBR (Australia) | I19S3c14 | 20°46'S | 150°53'E | 7 | 9.05 | 6.63 | 4.31 | 1.54 | 1.14 | 7.78 | 25.49 | 15.7 | < DL |
| Noumea Lagoon (New Caledonia) | I21S2c16 | 22°32'S | 166°26'E | 12 | 8.94 | 6.70 | 4.20 | 1.59 | 1.05 | 7.77 | 24.49 | 10.6 | < DL |
| E Vangunu (Salomon) | I22S2c1 | 08°36'S | 158° 11'E | 4 | 8.79 | 6.40 | 4.83 | 1.33 | 0.96 | 7.72 | 29.43 | 16.7 | < DL |
| E Vangunu (Salomon) | I22S2c2 | 08°36'S | 158° 11'E | 4 | 8.75 | 6.06 | 5.14 | 1.18 | 0.97 | 7.67 | 29.43 | 12.5 | < DL |
| Losuia, Tabungora Island (PNG) | I23S2 | 09°21'S | 152°02'E | 13 | 8.78 | 5.94 | 4.82 | 1.23 | 1.02 | 7.64 | 28.69 | 9.9 | < DL |
| Kimbe, Hoskins District (PNG) | I24S2c2 | 05°05'S | 150°12'E | 17 | 8.71 | 5.65 | 4.45 | 1.27 | 1.05 | 7.55 | 29.75 | 11.7 | < DL |
| N Hoskins District (PNG) | I24S3c22 | 05°12'S | 150°23'E | 6 | 8.73 | 5.66 | 4.64 | 1.22 | 1.05 | 7.56 | 29.76 | 16.3 | < DL |
| Helen Reef (Palau) | I25S1c1 | 02°57'N | 131°48'E | 3 | 8.83 | 5.84 | 4.48 | 1.30 | 1.07 | 7.63 | 29.32 | 10.6 | < DL |
| Helen Reef (Palau) | I25S1c2 | 02°57'N | 131°45'E | 9 | 8.78 | 5.70 | 4.30 | 1.33 | 1.09 | 7.57 | 29.32 | 11.6 | < DL |
| North Palau | I26S1c26 | 07°47'N | 134°35'E | 16 | 8.80 | 5.61 | 4.44 | 1.26 | 1.00 | 7.70 | 29.16 | 9.4 | 0.8 |
| Koror (Palau) | I26S2 cont 1 | 07°17'N | 134°21'E | 4 | 8.73 | 5.54 | 4.44 | 1.25 | 1.02 | 7.60 | 29.20 | 13.8 | < DL |
| Koror (Palau) | I26S2 cont 2 | 07°17'N | 134°21'E | 4 | 8.71 | 5.51 | 4.42 | 1.25 | 1.02 | 7.57 | 29.20 | 8.3 | < DL |
| Acidic site, Koror (Palau) | I26S2 acid | 07°19'N | 134°29'E | 4 | 8.79 | 5.37 | 4.25 | 1.26 | 1.07 | 7.60 | 29.19 | 14.1 | < DL |
| Green Island (Taiwan) | I28S3 | 22°39'N | 121°29'E | 3 | 8.86 | 5.59 | 4.01 | 1.39 | 1.07 | 7.67 | 26.82 | 8.1 | < DL |
| Clipperton (France) | I31S3 | 10°18'N | 109°12'W | 10 | 8.98 | 5.65 | 4.06 | 1.39 | 1.16 | 7.69 | 28.36 | 14.2 | < DL |
| Secas islands (Panama) | I32S1 | 07°57'N | 82°03'W | 3 | 8.83 | 5.60 | 4.86 | 1.15 | 1.01 | 7.71 | 28.96 | 11.8 | 0.8 |
| ***Diploastrea* spp.** | | | | | | | | | | | | | |
| Noumea Lagoon (New Caledonia) | I21S2c17 | 22°33'S | 166°26'E | 15 | 9.04 | 6.56 | 3.87 | 1.70 | 1.04 | 7.88 | 24.49 | 3.0 | < DL |
| Losuia, Tabungora Island (PNG) | I23S2 | 09°21'S | 152°02'E | 13 | 8.87 | 5.62 | 3.79 | 1.48 | 1.05 | 7.70 | 28.69 | 4.1 | 1.0 |
| Kimbe, Hoskins District (PNG) | I24S2c3 | 05°05'S | 150°12'E | 8 | 9,00 | 5.88 | 4.15 | 1.42 | 1.13 | 7.74 | 29.77 | 5.4 | < DL |
| W Garua, N Hoskins District (PNG) | I24S3c23 | 05°19'S | 150°07'E | 7 | 8.80 | 5.66 | 4.28 | 1.32 | 1.06 | 7.61 | 29.74 | 5,0 | < DL |
| North Palau | I26S1 | 07°47'N | 134°35'E | 16 | 8.76 | 6.00 | 4.68 | 1.28 | 0.96 | 7.70 | 29.16 | 5.1 | < DL |
| Green Island (Taiwan) | I28S3 | 22°39'N | 121°29'E | 13 | 8.95 | 5.75 | 3.53 | 1.63 | 1.11 | 7.73 | 26.82 | 6.3 | 1.4 |

### 3.2.3. SST and elemental proxy calibrations

All SST calibrations span ~ 7°C, from 22.4 ± 0.2°C to 29.8 ± 0.2°C. Fig. 7 shows linear regressions between ambient seawater temperature and coral Sr/Ca, Li/Mg, and Sr-U for the *Porites* and *Diploastrea* core-tops. The three temperature proxies were inversely correlated to the seawater temperature in the range between 22.4 ± 0.2°C and 29.8 ± 0.2°C for *Porites*, and 24.5 ± 0.2°C to 29.8 ± 0.2°C for *Diploastrea*. Regressions using different combinations of Sr/Ca, Li/Ca, Mg/Ca and Li/Mg were also tested to generate multi-ratio SST calibrations for both genera. The regression parameters and calibration equations are reported in Table 2. The RMSE values were calculated from the full 40 core-tops.

The Sr/Ca-SST regressions showed higher uncertainties (RMSE ranging from 0.99 to 1.90°C) than Li/Mg (RMSE ranging from 0.82 to 0.98°C) regardless of the genus considered. Overall, the variability of the prediction accuracy of the calculated SST was better when using the combination of Sr/Ca and Li/Mg (RMSE < 0.87 °C for *Porites*, *Diploastrea,* and multi-genera calibrations) compared to single Sr/Ca or Li/Mg calibrations (Table 2). For multi-species calibrations, the combination of Sr/Ca and Li/Mg or Sr/Ca, Li/Ca and Mg/Ca strengthened the relationship between the coral geochemical composition and SST (RMSE = 0.87 and 0.72 °C, respectively). This is particularly evident for *Diploastrea* that showed the lowest RMSE (0.19 °C) for Sr/Ca-Li/Ca-Mg/Ca proxy. Overall, multi-proxy calibrations revealed greater confidence in the SST reconstructions compared to single-ratio calibrations. These results are in line with recent studies that investigated the Sr/Ca-Li/Mg proxy, which improved the reliability of the SST reconstructions based on *Siderastrea* (Fowell et al., 2016) and *Porites* (D'Olivo et al., 2018; Zinke et al., 2019). The RMSE for the Sr-U *vs*. SST linear regressions (equation F, L, Q), which consider the Sr-U values derived from equation 4 in DeCarlo et al. (2016) (i.e., without using the correlation between Sr/Ca and U/Ca), ranged from 1.25 to 1.83 °C, and was higher than the uncertainty obtained by Ross et al. (2019) (0.92 °C) using a quadratic model in the temperature range ~ 18-30 °C. The general multi-species Sr-U calibration (equation G), which compiles data from this study with those from DeCarlo et al. (2016), Alpert et al. (2017), and Ross et al. (2019), showed an RMSE of 1.66 °C. The slope of the Sr/Ca calibration equation for *Diploastrea* (-0.045 ± 0.005) is significantly different from that of *Porites* (-0.073 ± 0.006) and multi-genera (-0.069 ± 0.005). This can be mainly explained by the low number of points available for *Diploastrea* (n = 6) compared to *Porites* (n = 34) and the narrower temperature range (5.3 °C *vs*. 7.4 °C for *Diploastrea* and *Porites* specific calibrations, respectively). Corrège et al. (2006) calculated a mean equation for *Porites* (Sr/Ca = -0.0607 SST + 10.553) based on a compilation of published calibrations obtained at sub-annual resolution from different sites, SST range, and SST sources (black dotted line, Fig. 7A). Despite the temporal scale (yearly *vs*. sub-annual), the slopes obtained in the present study (Eq. B and H) were similar, within error, to the general equation by Corrège et al. (2006). However, the slopes of equations B and H were partly controlled by the limited number of points at low temperatures (22-24

°C; n = 2) compared to warm temperatures (28-30 °C; n = 20), which slightly increased the slope values.

The Sr/Ca, Li/Mg, and Sr-U *vs*. SST regressions for *Diploastrea* (red line, Fig. 7) suffered from the limited number of samples and temperature range (from 24.5 to 29.8 °C). This could explain the difference in slope and intercept between our Sr/Ca *vs*. SST regression and that reported by Corrège et al. (2004) (Sr/Ca = - 0.060 SST + 10.57) for the same genus collected in Indonesia and New Caledonia, spanning a ~ 8 °C range (from 22 to 30 °C). However, this mismatch is also partly the result of the different regression models applied, ordinary least squares (Corrège et al., 2004) vs. weighted robust regression (this study). Indeed, the calibration equation calculated using the ordinary least squares is Sr/Ca = - 0.033 SST + 9.85.

The slopes of the Sr-U regressions were similar, within error, for *Porites* (-0.034 ± 0.005), *Diploastrea* (-0.036 ± 0.013), and multi-genera (-0.033 ± 0.005) but differed from the general Sr-U calibration (-0.058 ± 0.002, Eq. G) obtained by combining results from this study and literature values.

Overall, our geochemical analyses at yearly resolution using core-tops of *Porites* and *Diploastrea* collected from spatially distant sites in the Pacific Ocean indicate a strong sensitivity of Sr/Ca, Li/Mg, and Sr-U to temperature, especially for the combined Sr/Ca-Li/Mg.

441 **Table 2**

442 Regression parameters of the SST calibrations developed in this study. (*) calibration G was obtained
443 by combining Sr-U values from the present study and from DeCarlo et al. (2016), Alpert et al. (2017)
444 and Ross et al. (2019).

| Calibration | Proxy | Calibration equation | RMSE (°C) |
|---|---|---|---|
| Multi-genera | Sr/Ca | (B) Sr/Ca = -0.069 SST + 10.78 | 1.19 |
| | Li/Mg | (C) Li/Mg = -0.084 SST + 3.74 | 0.98 |
| | Sr/Ca-Li/Mg | (D) SST = 68.50 - 3.47 Sr/Ca - 7.09 Li/Mg | 0.87 |
| | Sr/Ca-Li/Ca-Mg/Ca | (E) SST = 50.82 - 1.63 Sr/Ca - 2.87 Li/Ca + 2.03 Mg/Ca | 0.72 |
| | Sr-U | (F) Sr-U = -0.033 SST + 8.63 | 1.83 |
| | Sr-U (*) | (G) Sr-U = -0.058 SST + 9.39 | 1.66 |
| *Porites* spp. specific | Sr/Ca | (H) Sr/Ca = -0.073 SST + 10.91 | 0.99 |
| | Li/Mg | (I) Li/Mg = -0.087 SST + 3.79 | 0.82 |
| | Sr/Ca-Li/Mg | (J) SST = 60.80 - 2.48 Sr/Ca - 7.94 Li/Mg | 0.74 |
| | Sr/Ca-Li/Ca-Mg/Ca | (K) SST = 50.66 - 1.65 Sr/Ca - 2.79 Li/Ca + 1.98 Mg/Ca | 1.08 |
| | Sr-U | (L) Sr-U = -0.034 SST + 8.63 | 1.77 |
| *Diploastrea* spp. specific | Sr/Ca | (M) Sr/Ca = -0.045 SST + 10.14 | 1.90 |
| | Li/Mg | (N) Li/Mg = -0.071 SST + 3.48 | 0.96 |
| | Sr/Ca-Li/Mg | (O) SST = -3.90 + 5.97 Sr/Ca - 14.34 Li/Mg | 0.77 |
| | Sr/Ca-Li/Ca-Mg/Ca | (P) SST = -46.66 + 10.34 Sr/Ca - 6.33 Li/Ca + 4.96 Mg/Ca | 0.19 |
| | Sr-U | (Q) Sr-U = -0.036 SST + 8.75 | 1.25 |

445

### 3.3. *Porites* and *Diploastrea* colonies of Palau

#### 3.3.1. Age model

The X-ray radiography and the computed tomography (CT-scan) of both *Porites* and *Diploastrea* long-cores from Palau (I26S1) showed a density-banding pattern (Fig. 4). The mean linear extension rates were 10.7 ± 0.2 mm·yr$^{-1}$ and 5.7 ± 0.4 mm·yr$^{-1}$ for *Porites* and *Diploastrea* colonies, respectively. The values for *Porites* were similar to those reported by van Woesik et al. (2015) and DeCarlo (2017) (7.3 to 13.4 mm·yr$^{-1}$), but lower than those reported by Osborne et al. 2013 (13.6 to 20.5 mm·yr$^{-1}$) for the same genus at the same location. Along both colonies, skeletal banding was unclear in some coral portions, most likely as the result of the narrow seasonal amplitude (~ 1.5 °C, Osborne et al., 2013) in the sampling location that reduced the coral density contrast between summer and winter. For this reason, the U/Th dating method was applied to both colonies and confirmed the age model obtained by sclerochronology. The initial $\delta^{234}U$ ratio of the samples ($\delta^{234}U_i$) is within the expected value for seawater and modern corals ($\delta^{234}U$ = 145 ± 1.5, Chutcharavan et al., 2018). Due to the low $^{232}Th$ concentration (< 0.1 ng·g$^{-1}$) and high $^{230}Th/^{232}Th$ ratio (> 19), the detrital correction had a negligible effect (Table 3). Corrected ages ranged between the years 2014 ± 3 and 1968 ± 4 for the *Porites* colony and between the years 2014 ± 3 and 1883 ± 12 for the *Diploastrea* colony. These ages were consistent, within error, with our sclerochronological model obtained by annual band counting (Table 3).

**Table 3**

Uranium and thorium concentrations, isotopic composition and ages of coral samples. The uranium isotopic ratio is expressed as $\delta^{234}U = ([^{234}U/^{238}U] - 1) \times 1000)$. Errors are given at 2σ absolute uncertainties. The initial $\delta^{234}U$ value ($\delta^{234}U_i$) was calculated based on $^{230}Th$ age (T), i.e., $\delta^{234}U_i = \delta^{234}U_m e^{\lambda 234 T}$, where $\delta^{234}U_m$ is the measured $\delta^{234}U$. Ages are given as raw age (Age) and ages corrected for detrital fraction (Corrected Age) as ka before the analysis (year 2018). Corrected ages are also reported as calendar ages.

| Sample | $[^{238}U]$ ppm | $[^{232}Th]$ ppb | $\delta^{234}U_m$(‰) | $(^{230}Th/^{238}U)$ | $(^{230}Th/^{232}Th)$ |
|---|---|---|---|---|---|
| I 26 P - Middle | 2.338 ± 0.019 | 0.0299 ± 0.0002 | 146.6 ± 0.8 | 0.00032 ± 0.00002 | 75.8 ± 4.8 |
| I 26 P - Bottom | 2.362 ± 0.019 | 0.0221 ± 0.0002 | 144.2 ± 0.6 | 0.00055 ± 0.00002 | 178.3 ± 8.0 |
| I 26 D - Top | 2.174 ± 0.018 | 0.0256 ± 0.0002 | 145.8 ± 1.0 | 0.00008 ± 0.00002 | 19.4 ± 5.1 |
| I 26 D - Middle | 2.223 ± 0.018 | 0.0186 ± 0.0002 | 145.5 ± 1.2 | 0.00093 ± 0.00005 | 338.3 ± 17.0 |
| I 26 D - Bottom | 2.577 ± 0.021 | 0.0988 ± 0.0009 | 143.8 ± 1.5 | 0.00153 ± 0.00007 | 120.7 ± 6.0 |

| Sample | Age (ka) | $\delta^{234}U_i$(‰) | Corrected Age (ka) | Calendar Age (AD) | Age from sclerochronology (AD) |
|---|---|---|---|---|---|
| I 26 P - Middle | 0.031 ± 0.002 | 146.6 ± 0.8 | 0.027 ± 0.004 | 1991 ±4 | 1989 |
| I 26 P - Bottom | 0.053 ± 0.002 | 144.2 ± 0.6 | 0.051 ± 0.004 | 1968 ±4 | 1970 |
| I 26 D - Top | 0.008 ± 0.002 | 145.8 ± 1.0 | 0.004 ± 0.003 | 2014 ±3 | 2016 |
| I 26 D - Middle | 0.090 ± 0.005 | 145.5 ± 1.2 | 0.087 ± 0.006 | 1932 ±5 | 1928 |
| I 26 D - Bottom | 0.147 ± 0.007 | 143.8 ± 1.5 | 0.135 ± 0.012 | 1883 ±12 | 1874 |

### 3.3.2. Elemental ratios

Minima, maxima and mean values of the elemental ratios obtained from the *Diploastrea* (1874-2016) and the *Porites* (1970-2016) long cores are presented in table 4. Overall, *Diploastrea* showed slightly higher Li/Ca, Mg/Ca, and Li/Mg values than those of *Porites* (mean values: + 15.4 % for Li/Ca, + 5.3 % for Mg/Ca, + 10.2 % for Li/Mg) and slightly lower Sr/Ca, U/Ca and Sr-U values (– 1 % for Sr/Ca, – 4.2 % for U/Ca and – 0.5 % for Sr-U).

**Table 4**

Minima, maxima and mean (± 1σ SD) values for Sr/Ca, Li/Ca, Mg/Ca, Li/Mg, U/Ca and Sr-U in *Porites* (n = 88) and *Diploastrea* (n = 323) cores from Palau (I26S1).

| | | *Porites* spp. | | | | *Diploastrea* spp. | | | |
|---|---|---|---|---|---|---|---|---|---|
| | | Min | Max | Mean | ± 1SD | Min | Max | Mean | ± 1SD |
| Sr/Ca | $mmol \cdot mol^{-1}$ | 8.76 | 8.97 | 8.88 | 0.04 | 8.63 | 8.93 | 8.79 | 0.04 |
| Li/Ca | $\mu mol \cdot mol^{-1}$ | 4.71 | 5.42 | 5.06 | 0.16 | 5.57 | 6.38 | 5.98 | 0.14 |
| Mg/Ca | $mmol \cdot mol^{-1}$ | 3.90 | 4.94 | 4.45 | 0.23 | 4.36 | 5.05 | 4.70 | 0.12 |
| Li/Mg | $mmol \cdot mol^{-1}$ | 1.04 | 1.23 | 1.14 | 0.05 | 1.19 | 1.33 | 1.27 | 0.02 |
| U/Ca | $\mu mol \cdot mol^{-1}$ | 0.95 | 1.06 | 0.99 | 0.02 | 0.90 | 1.01 | 0.95 | 0.02 |
| Sr-U | | 7.68 | 7.85 | 7.78 | 0.03 | 7.62 | 7.84 | 7.74 | 0.04 |

# 4. Discussion

## 4.1. Sources of uncertainties of SST calibrations

The quality of the coral-based calibrations used to reconstruct past seawater temperatures depends on different factors, including the presence of calcite, organic matter, and other diagenetic products (e.g., secondary aragonite), the analytical uncertainty, and the choice of the SST database used for the calibrations. Regression uncertainty is usually calculated based on the discrepancy between reconstructed and measured SST.

### 4.1.1. Impact of the analytical uncertainty on SST reconstructions

The analytical precision of ICP-QMS calculated from repeated JCp-1 and M1P-p measurements (*cf.* 2.5.2), without considering the regression errors, resulted in SST uncertainties ranging from 0.9 °C (Eq. H) to 1.4 °C (Eq. M) for the Sr/Ca proxy and from 0.3 °C (Eq. I) to 0.4 °C (Eq. N) for Li/Mg. SST uncertainties based on multi-ratios ranged from 0.4 °C (Eq. J) to 0.8 °C (Eq. O) for Sr/Ca-Li/Mg and from 0.6 °C (Eq. K) to 1.8 °C (Eq. P) for Sr/Ca-Li/Ca-Mg/Ca, and increased to 2.4 °C for all Sr-U equations, except for equation G (1.4 °C). In general, the impact of analytical uncertainties on the SST reconstruction is substantial, accounting for half of the total uncertainty. Although the analytical precision can contribute significantly to the overall SST uncertainty, depending on the instrument used and analytical protocol applied, other sources of uncertainty (e.g., the presence of calcite or organic matter) may have a larger impact and need to be carefully considered.

### 4.1.2. Presence of calcite and organic matter

The geochemical signature of the aragonite skeleton of modern corals can be altered by different early and post-depositional diagenetic processes, including bioerosion, dissolution, secondary aragonite and calcite precipitation, replacement of aragonite by calcite, or the presence of organic matter, as in the green bands often observed in tropical corals (Macintyre and Towe, 1976; McGregor and Gagan, 2003; Hendy et al., 2007; Nothdurft and Webb, 2009; Lazareth et al., 2016; Cuny-Guirriec et al., 2019). In particular, early diagenetic intra-skeletal calcite has a lower Sr/Ca and Li/Mg composition than that of skeletal aragonite (Sayani et al., 2011; Lazareth et al., 2016), significantly impacting the temperature reconstructions, and could explain part of the uncertainties associated to our calibrations. A previous study has shown that diagenetic calcite in fossil tropical corals can bias Sr/Ca-based reconstructions by 1.1 to 1.5 °C per percent calcite (McGregor and Gagan, 2003). In modern tropical corals, Lazareth et al. (2016) showed that 1 % of calcite in coral skeleton equals a temperature bias varying from + 0.08 °C to + 0.26 °C, based on Sr/Ca and Li/Mg proxies, respectively. However, Lazareth et al. (2016) concluded that the presence of less than 5 % of intra-skeletal calcite does not significantly impact SST reconstructions based on Sr/Ca. Considering the higher sensitivity of Li/Mg proxy to the amount of calcite ($0.26°C·\%^{-1}$) (Lazareth et al., 2016), we estimate a 4 % of calcite as a

reasonable upper limit for reliable (± 1°C) SST reconstructions using the Li/Mg proxy. Our samples do not display a significant correlation between the level of calcite and ΔT ($T_{coral}$-$T_{OiSST}$). In particular, the highest percentage of calcite (3.6 %) measured in the *Porites* colony from Guam does not correspond to the largest ΔT (-3.9 °C and 4.4 °C for Sr/Ca and Li/Mg, respectively), which is observed for the *Diploastrea* colony from PNG (I24S2), showing calcite level below the detection limits.

Except for the *Porites* from Guam, only 5 core-top samples have a calcite percentage between the DL (0.6 %) and 1.4 %. This means that 85 % of our samples are characterized by calcite values lower than DL, which highlights the aragonite quality of the core-top samples used to derive the calibrations. Figure 7 shows that samples with calcite levels above the DL mostly plot along the regression lines and their Sr/Ca, Li/Mg and Sr-U values are not distinguishable from samples with calcite level < DL. These results demonstrate that the influence of small amounts of calcite within the skeleton on the overall uncertainty of our calibration equations is minimal. In addition, the core-tops of the *Porites* and *Diploastrea* colonies did not show any visible bands related to the presence of endolithic green algae, which may lead to temperature overestimation when using the Li/Mg proxy (Cuny-Guirriec et al., 2019). Moreover, the application of a specific oxidative cleaning protocol (Cuny-Guirriec et al., 2019) to all coral samples prior to the geochemical analysis ensured the complete removal of any organic material residues.

### 4.1.3. Reproducibility of coral skeleton geochemical data

**Intra-colony geochemical variability**

Like all proxy calibrations, those involving corals necessitate a precise alignment of the timing of coral skeletal growth with the corresponding environmental parameter (e.g., SST). Our calibrations were performed by comparing the mean SST value for the period 2010-2016 with the mean Sr/Ca, Li/Ca, Mg/Ca, Li/Mg, and Sr-U values of the corresponding period of skeletal growth, as determined by the banding pattern. The primary uncertainty of this approach stems from the sampling and analysis of the coral portion, along with the concern that it precisely reflects the mean geochemical composition over the more recent six years of growth. In order to assess this uncertainty, we collected 3 sub-samples representing the final 6 years of growth from 3 distinct *Porites* cores (I5S4, I21S2c16, I22S2c2) living at SST between ~ 22 °C and ~ 30 °C, and a *Diploastrea* colony (I21S2c17) living at ~ 24 °C. The reconstructed SST for the four selected sites based on single- and multi-proxy and multi-genera calibrations are plotted in figure 8. In general, the reproducibility between the triplicates for each core and each proxy is high, with the relative standard deviations (RSD) ranging from 0.2 % to 2.8 %. In particular, the Sr-U and the Li/Mg proxy showed the lowest (~ 0.9 %, blue dots) and the highest (~ 2 %, yellow dots) mean RSD, respectively. For *Porites*, the RSD is generally larger when applying the Li/Mg calibration (~ 2.3 %) and lower when using Sr/Ca (~ 1%, purple dots). Overall, the intra-colony reproducibility is high for both genera and for all proxies. This provides further evidence that both genera can serve as reliable archives for SST reconstructions. Additionally, it suggests that

554 bulk sampling of *Diploastrea* is a reproducible method and can help reduce the geochemical
555 variability associated with various skeletal microstructures (Watanabe et al., 2003; Bagnato et al.,
556 2004).
557 The mean reconstructed SST values (average of the triplicates) match well with the ambient
558 temperatures obtained from the AVHRR-OISSTv2 database, with differences (ΔT) being generally
559 lower than 0.5°C, except for the Sr-U proxy (ΔT = 2.1 ± 1.6 °C). Overall, multi-ratios Sr/Ca-Li/Mg
560 (green dots) and Sr/Ca-Li/Ca-Mg/Ca (orange dots) calibrations yield the most accurate SST estimates,
561 whether using genus-specific or multi-genera calibrations. These results confirm recent studies that
562 highlighted the benefit of multi-ratio proxies in SST reconstructions (Fowell et al., 2016; D'Olivo et
563 al., 2018; Zinke et al., 2019).
564
565 **Genus-specific effect**
566 The limited number of *Diploastrea* samples available for the present study may partly explain the
567 difference in the individual-specific Sr/Ca calibration slopes between *Diploastrea* (-0.045 ± 0.005) and
568 *Porites* (-0.073 ± 0.006) (Fig. 7A; Table 2). Once the regression model combines the Sr/Ca values
569 from both genera, the resulting multi-genera slope (-0.069 ± 0.005) is similar to those reported in
570 Corrège et al. (2004) for *Diploastrea* (-0.060) and *Porites* (-0.062). However, to properly assess
571 individual-specific calibrations and potential inter-genus effects, it would be necessary to include
572 additional *Diploastrea* specimens.
573 The regression slopes for the Li/Mg-SST calibrations are similar, within error, for *Diploastrea* (-0.071
574 ± 0.019) and *Porites* (-0.087 ± 0.006) (Fig. 7B, Table 2), supporting previous findings showing the
575 species independent character of the Li/Mg temperature proxy (e.g. Hathorne et al., 2013; Montagna et
576 al., 2014; Marchitto et al., 2018; Cuny-Guirriec et al., 2019). However, small differences exist
577 between *Diploastrea* and *Porites* in the Li/Mg values, especially for warmer temperatures (Fig. 7B).
578 The Sr-U vs. SST relationships exhibit some variations across the different datasets, as evidenced in
579 figure 7-C. This underscores an existing knowledge gap in the Sr-U thermometry that can be
580 addressed by expanding the analysis of Sr/Ca and U/Ca in more shallow-water coral specimens from
581 other regions and eventually exploring the application of this method in azooxanthellate corals in
582 future studies.
583 For the multi-ratio proxies (Sr/Ca-Li/Mg and Sr/Ca-Li/Ca-Mg/Ca), the comparison of calibration
584 equations (Table 2) clearly indicates that regression parameters of *Porites* and multi-genera
585 calibrations are very similar. On the contrary, the low number of samples (6 *vs*. 34) and the narrower
586 temperature range covered by the *Diploastrea* specimens (22.4-29.8°C *vs*. 24.5-29.8°C) represent a
587 limitation when building the regression models. Additional *Diploastrea* samples would be required to
588 confirm potential species/genus effects on the geochemical proxies.

### 4.1.4 Gridded and *in-situ* temperature data: spatial resolution and depth gradient

SST data for proxy calibrations are typically derived from a combination of observations by satellites, ships, and buoys (e.g. HadlSST, ERSST, AVHRR-OISST), which provide data at a spatial resolution of 1/4° to 2°, or from direct *in situ* measurements by temperature sensors (Corrège, 2006; Pfeiffer et al., 2017; D'Olivo et al., 2018).

A potential source of error in proxy calibration arises from the discrepancy between the actual temperature experienced by the coral throughout its lifespan and the temperature selected for the calibration. *In-situ* temperatures are usually the best approach because the temperature sensor is close to the coral colony and reflects the ambient temperature of the reef. Unfortunately, few sparse *in-situ* SST measurements are available for most of the coral sites explored by the Tara Pacific expedition, which prevents a complete assessment of the quality of the AVHRR-OISSTv2 dataset for the study sites. In addition, satellite-based data represent the surface temperature (10-20 μm to 1 mm below the surface), while zooxanthellate corals can live from the surface to ~ 100-150 m water depth (e.g., Englebert et al., 2014). Coral samples from the Tara Pacific expedition were collected from 3 to 20 m depth (Table 1). To quantify the seawater temperature variability with depth, we calculated the mean difference in monthly *in-situ* temperature at 2 m and 15 m over the period 2000-2018 at the Short Drop Off site in Palau, which is ~ 55 km from the Ebiil Channel site (Palau, Fig. 2). Unfortunately, depth profiles of temperature in the Ebiil Channel are not available. On average, the upper layer is 0.1 °C warmer than the 15 m deep layer. We also calculated the temperature-depth gradient (0-10 m) for the different Tara Pacific sampling locations using the World Ocean Atlas 2018 (Locarnini et al., 2018). The mean value (-0.11 ± 0.04 °C / 10 m) is consistent with the *in-situ* value in Palau. Applying this gradient to our sampling sites results in a maximum difference of 0.22 °C between the AVHRR-OISSTv2 value and the temperature of the deepest coral colony (CSR 11, Wallis). Although the difference between the *in-situ* temperature and the temperature of the dataset may contribute to the overall uncertainty of the proxy calibration, this seems to play a minor role compared to the analytical uncertainty, intra-colony geochemical variability, and the presence of calcite or organic matter.

## 4.2 SST reconstructions in Palau

### 4.2.1 *Porites* and *Diploastrea* records over the period 1982-2016

The SST reconstructions based on the *Porites* and *Diploastrea* long cores from Palau were compared to the AVHRR-OISSTv2 dataset for the period 1982-2016 to evaluate the performance of the basin-wide general calibration equations and assess the potential of both genera in reliably reconstructing the SST variations.

Figure 9 shows the reconstructed SST based on the different single- and multi-ratio calibrations for *Porites* and *Diploastrea.* Mean values for the 1982-2016 period obtained from the *Porites* colony range from 27.7 ± 0.6 to 31.0 ± 0.5 °C and are significantly different (one-way ANOVA) from AVHRR-OISSTv2 (28.78 ± 0.4 °C). In particular, the Sr/Ca proxy in *Porites* underestimates the ambient temperature by 1.09 and 0.98 °C when using the multi-genera and the *Porites*-specific calibrations, while Li/Mg and multi-ratio calibrations tend to overestimate the temperature by 0.98 to 2.36 °C (Fig. 9). For the *Diploastrea* colony, temperatures derived from the multi-genera calibrations are more accurate, especially when applying the multi-ratio approach (Eq. D, E, G, green boxplots in figure 9). On the other hand, all *Diploastrea*-specific calibrations overestimate the mean SST, reinforcing the argument that the limited dataset for *Diploastrea* necessarily compromises the performance of the calibrations. Overall, these results show that the multi-genera equations applied to *Diploastrea* provide the most accurate and precise reconstruction of the mean SST value.

SST variability reconstructed at sub-annual resolution in Palau over the 1982-2016 period from *Porites* (Fig. 10A, C) and *Diploastrea* (Fig. 10B, D) is shown together with the AVHRR-OISSTv2 time series (black lines). *Porites*-based reconstructions spread over an amplitude range of ~ 3-4 °C when applying both genus-specific and multi-genera calibrations. The derived time-series show some coherence among SST reconstructions regardless of the proxy considered, but absolute SST values are quite different. The *Diploastrea*-derived records (Fig. 10B) are consistent with the OISST time-series in terms of absolute temperature and SST variations, whereas *Porites* shows a larger SST range (Fig. 10A). The SST variability obtained from the Sr/Ca (Eq. B) and Sr-U (Eq. G) equations in *Diploastrea* exceeds that derived from other proxies and OISST.

According to the AVHRR-OISSTv2 and ERSSTv5 datasets, sea surface temperature in Palau warmed by 0.23 ± 0.04 °C and 0.18 ± 0.04 °C per decade respectively, during the 1982-2016 period. Over the same period, sub-annual SST derived from *Porites* showed warming trends between 0.07 ± 0.06 and 0.09 ± 0.07 °C per decade, for Sr/Ca-Li/Ca-Mg/Ca and Li/Mg-derived SST, respectively (Table 6). Although these trends are similar within error, they are not significant ($p$-value > 0.05, Mann-Kendall test).

On the contrary, sub-annual SST records derived from *Diploastrea* display varied trends, ranging from – 0.08 ± 0.04 to 0.22 ± 0.12 °C per decade for Li/Mg and Sr/Ca proxy, respectively (Table 6). Significant SST trends ($p$-value < 0.001, Mann-Kendall test) were calculated using multi-genera Sr/Ca

(0.15 ± 0.08 °C per decade) and Sr-U (0.14 ± 0.08 °C per decade) equations. A significant warming trend was also obtained using the genus-specific Sr/Ca equation (0.22 ± 0.12 °C per decade). These trends are similar within error to those calculated from OISST (0.23 ± 0.04 °C per decade) or ERSSTv5 (0.18 ± 0.04 °C per decade) datasets (Table 6). All the other SST reconstructions derived from *Diploastrea* did not reveal significant trends. When applying the multi-genera calibrations to *Diploastrea*, all proxies, with the exception of Li/Mg, show positive trends, as high as 0.15 ± 0.08 °C per decade for Sr/Ca ($p$-value < 0.001, Mann-Kendall test). On the other hand, SST trends derived from *Diploastrea*-specific calibrations are negative (except for Sr/Ca). These results highlight the limitations of the specific equations for *Diploastrea* and underscore the necessity for a more extensive sample collection to improve the quality of the SST calibrations for this genus. Overall, comparison of the *Porites* results reveals that most of the trends reconstructed from single- or multi-ratio calibrations are consistent, though not statistically significant and much weaker than those derived from OISSTv2 and ERSSTv5. On the other hand, the Sr/Ca-derived SST from *Diploastrea* shows surface warming in Palau similar to previous observations for the western Pacific Ocean (Tierney et al., 2015).

**Table 6**

Reconstructed SST trends (°C per decade) from 1982 to 2016 in Palau based on the *Porites* and *Diploastrea* SST calibrations developed in this study (Table 2). Uncertainties (1σ SE) are reported in parenthesis. "*" represents significant trends ($p$-value < 0.001, Mann-Kendall trend test).

| | | 1982 - 2016 | |
|---|---|---|---|
| Calibration | Proxy | *Porites* sp. | *Diploastrea* sp. |
| Multi-genera | Sr/Ca | + 0.082 (*73*) | + 0.146 (*81*) * |
| | Li/Mg | + 0.094 (*74*) | - 0.016 (*28*) |
| | Sr/Ca-Li/Mg | + 0.076 (*50*) | + 0.025 (*28*) |
| | Sr/Ca-Li/Ca-Mg/Ca | + 0.069 (*63*) | + 0.035 (*31*) |
| | Sr-U (*) | + 0.072 (*67*) | + 0.136 (*84*) * |
| Genus-specific | Sr/Ca | + 0.078 (*69*) | + 0.224 (*124*) * |
| | Li/Mg | + 0.090 (*71*) | - 0.019 (*33*) |
| | Sr/Ca-Li/Mg | + 0.076 (*53*) | - 0.080 (*41*) |
| | Sr/Ca-Li/Ca-Mg/Ca | + 0.067 (*62*) | - 0.074 (*87*) |
| AVHRR-OISSTv2 | | + 0.227 (*39*) * | |
| ERSSTv5 | | + 0.181 (*40*) * | |

The large variation in the reconstructed SST based on the different proxies/equations used in the *Porites* colony (Fig. 10A) suggests biases possibly related to the influence of calcification processes in the incorporation of minor and trace elements in the coral skeleton. We tentatively explored the possibility that coral heterogenous growth dynamics at microscale (reflected as differences in two main microstructural units; see Stolarski, 2003; Brahmi et al., 2012) is partly driving the difference in elemental composition between *Porites* and *Diploastrea*. The hypothesis was tested through the quantification of skeletal regions composed of Rapid Accretion Deposits (RAD's, referred also as centers of calcification) *vs*. Thickening Deposits (TD's, referred also as fibers) in two specimens of both genera. In well-developed skeletal portions, *Porites* showed higher RAD's/TD's ratio compared to *Diploastrea* (Figs 11 and 12), with percentage of RAD's varying between 6 and 11 % of the bulk skeleton. Instead, the skeleton of *Diploastrea* is mainly composed of TD's, with less than 2 % of RAD's (Figs 11 and 12). A higher proportion of RAD's vs TD's could lead to higher concentrations of elements such as Mg, Li, and Ba (and to a lesser degree Sr) and lower concentrations of B and U, given that these elements are enriched and depleted, respectively, in RAD's (Allison, 1996; Meibom et al., 2006; Sinclair et al., 2006; Case et al., 2010; Montagna et al., 2014). However, a difference in Li/Ca and Mg/Ca exists between the fast-growing RAD's and TD's, with Mg/Ca being relatively more enriched than Li/Ca in RAD's due to a higher growth rate dependence of the partition coefficient of Mg/Ca (Montagna et al., 2014). This results in a slightly lower Li/Mg (or higher Mg/Li) ratio in RAD's (Case et al., 2010; Montagna et al., 2014). The lower Li/Mg observed in our *Porites* samples compared to *Diploastrea* collected from the same environmental conditions (Fig. 7) is likely linked to microscale growth dynamics differences between the two genera. The higher RAD's/TD's ratio in *Porites* could also explain the larger scatter of SST reconstructed from different proxies (Fig. 10).

Other physiochemical parameters, including the different mechanisms through which seawater and ions are transported into the calcifying fluid of corals (e.g. active and passive transport of ions via diffusion, paracellular pathways, and $Ca^{2+}$-ATPase pump) or the distinct species-specific mechanisms used by corals to regulate their calcifying fluid chemistry can have an impact on the elemental incorporation (Gaetani and Cohen, 2006; Gagnon et al., 2007; Gaetani et al., 2011; Ross et al., 2019; Ram and Erez, 2021, 2023). However, these aspects are outside the scope of our study and, as such, will not discuss further.

### 4.2.2 Long-term SST variations from 1874 to 2016

Long-term records, such as the one derived from the *Diploastrea* colony of Palau, offer additional information to test the applicability of the universal calibrations developed in this study to capture decadal changes. Figure 13 shows the SST records spanning from 1874 to 2016, based on the *Diploastrea* colony of Palau and expressed as the deviation from the baseline period 1961-1990 period (Rayner et al., 2003). These reconstructions are derived from the multi-genera calibrations (e.g. Eq. B, C, D, E, G), as previously demonstrated to be the most reliable equations.

The Sr/Ca and Sr-U proxies provide similar patterns and both show a significant SST increase since 1874 ($p$-value < 0.001, Mann-Kendall trend test). However, the Sr-U thermometry exhibits greater amplitude variations and a slightly higher warming trend than Sr/Ca (0.08 ± 0.01 vs. 0.06 ± 0.01 °C per decade). Both proxies reveal negative anomalies from 1880 to 1900 and positive anomalies in the more recent years (1996-2016). In contrast, the ERSSTv5 dataset indicates positive anomalies in both periods and a moderate warming trend of 0.03 ± 0.01 °C per decade since 1874. The Li/Mg record shows a distinct warming phase around 1895, yet it also reveals a negative long-term trend ($p$-value = 0.005, Mann-Kendall trend test), which does not align with that derived from the ERSSTv5 dataset. However, considering the uncertainties and potential biases associated with historical changes in the ERSSTv5 data, especially at local grid scale and before 1900 (Huang et al., 2019), the warming event around 1895 should be regarded with caution and comparison with our pre-1900 *Diploastrea* records should be minimized.

Unlike the Sr/Ca-Li/Ca-Mg/Ca record, which predominantly shows positive SST anomalies throughout the entire period, the Sr/Ca-Li/Mg record aligns more closely with the long-term variability of ERSSTv5 at interannual to decadal scales, displaying similar amplitudes and warming-cooling phases (Fig. 13).

Based on these findings, it is clear that the long-term SST anomaly records from corals are influenced by the choice of proxies and calibrations, particularly in relation to linear trends and amplitude variations. The observed discrepancies between the coral records and the dataset might also stem from the mesoscale variability in the Palau archipelago, as opposed to the broader regional scale encompassed by the ERSSTv5 dataset. Nonetheless, our results suggest that *Diploastrea*-based reconstructions in Palau are well suited for exploring questions on the multi-decadal climate variability across the broad region of the Western Pacific Warm Pool (WPWP). Our study highlights the complexity of using trace elements in corals as absolute temperature proxies and indicates that relying on a single tracer might preferentially favor one biomineralization-related process over others. This reflects the significance of selecting appropriate chemical proxies for reconstructing past SST, thereby emphasizing the need to deepen our understanding of the mechanisms involved in the incorporation of these chemical elements into the coral skeleton and to accurately quantify their impact on temperature reconstructions.

## 5. Conclusions

Annual SST calibrations developed in this study using a unique dataset of 40 massive coral cores of *Porites* and *Diploastrea* collected during the Tara Pacific expedition across the Pacific Ocean show a notable reduction in uncertainties when applying a multi-element approach (e.g., Sr/Ca-Li/Mg), in line with recent works on *Siderastrea* in the Caribbean Sea (Fowell et al., 2016) and *Porites* in the Great Barrier Reef and Indian Ocean (D'Olivo et al., 2018; Zinke et al., 2019). Calibrations obtained through the Sr-U thermometry method (using equation 4 in DeCarlo et al., 2016) show a strong correlation with temperature (Eq. G, L and Q) but uncertainties are still higher (RMSE = 1.25-1.77 °C) than those calculated from the other multi-element calibrations. These results indicate that the combined systematics of Sr/Ca, Li/Ca, Mg/Ca, and/or Li/Mg significantly improve the reliability of the reconstructed mean annual temperature. However, additional studies are needed to employ Sr-U as a thermometer in corals, especially when using the approach that does not consider the interaction term (equation 4 in DeCarlo et al., 2016). The Sr-U thermometer holds potential as an alternative method to reconstruct SST, as the combined use of Sr/Ca and U/Ca measurements effectively reduces the impact of "vital effects". Advancements in analytical techniques, particularly in the measurement of Sr/Ca, Li/Ca and U/Ca ratios, could greatly improve the application of these novel multi-element SST proxies.

The calibrations were then applied to two long cores of *Porites* and *Diploastrea* to reconstruct the SST variability in Palau over the last decades. This study highlights the complexity and limitations in using coral geochemical proxies, revealing that the reliability of these proxies varies between different coral colonies. In particular, the *Porites* colony in Palau exhibits significant deviations in temperature reconstructions, suggesting that factors other than temperature alter the geochemistry of the coral skeleton. These discrepancies observed in the *Porites* records could be attributed to biological influences during biomineralization, such as the high ratio between the Rapid Accretion Deposits (RAD's) and the Thickening Deposits (TD's) in the skeleton, which impacts the incorporation of trace elements.

Conversely, the *Diploastrea* colony provides more accurate SST records in terms of absolute temperature, amplitude variations and short-term trends when applying multi-genera and multi-element calibrations (Eq. O, P, Q).

Collectively, the robustness of the calibration equations (Table 2) and the evaluation of the long-term SST reconstructions in Palau corroborate two key points: (1) the effectiveness of a multi-element approach (such as Sr/Ca-Li/Mg, Sr/Ca-Li/Ca-Mg/Ca-Li/Mg, and Sr-U), particularly for *Diploastrea*, which was used for the first time in this study, and (2) the relevance of using universal multi-genera calibrations to obtain robust temperature reconstructions at sub-annual resolution. This approach tends to minimize species-specific effects and reduces potential biases of single-ratio calibration, improving reconstructions from fossil tropical corals for which no current calibrations exist, like *Diploastrea*.

## Data Availability

Raw data are available on the journal website in electronic annexes.

## Acknowledgments

We greatly acknowledge the logistic and scientific support of the local and regional collaborators from the Pacific Island countries where the coral sampling was conducted. A complete list of the institutions, responsible people, and sampling permits is provided in the Supplementary Material.
Special thanks to the Tara Ocean Foundation, the R/V Tara crew and the Tara Pacific Expedition Participants (https://doi.org/10.5281/zenodo.3777760). We are keen to thank the commitment of the following institutions for their financial and scientific support that made this unique Tara Pacific Expedition possible: CNRS, PSL, CSM, EPHE, Genoscope, CEA, Inserm, Université Côte d'Azur, ANR, agnès b., UNESCO-IOC, the Veolia Foundation, the Prince Albert II de Monaco Foundation, Région Bretagne, Billerudkorsnas, AmerisourceBergen Company, Lorient Agglomération, Oceans by Disney, L'Oréal, Biotherm, France Collectivités, Fonds Français pour l'Environnement Mondial (FFEM), Etienne Bourgois, and the Tara Ocean Foundation teams. Tara Pacific would not exist without the continuous support of the participating institutes. The authors also particularly thank Serge Planes, Denis Allemand, and the Tara Pacific consortium.
We are grateful to the Ateliers Saint-Jacques in Saint-Rémy-les-Chevreuses for the coral cuttings, the Center of radiology in Gif-sur-Yvette for assistance in scanning the corals, Anne-Catherine Simon for the use of the CT scanner at the Doseo Platform (CEA-Saclay), Florence Le Cornec for the use of the automatic sampling system of the Institut de Recherche pour le Développement (IRD Bondy) and Patrick Colin for providing *in situ* SST around Palau Island from the Coral Reef Research Foundation (Palau). XRD measurements were performed at the ALYSES facility (IRD, Sorbonne University), that was supported by grants from Région Ile-de-France. Special thanks are due to David Monmarché and Jonathan Lancelot for their help during drilling. ICPMS measurements were performed at the PANOPLY platform (Paris-Saclay University). This work was supported by grants from the CEA-CSM convention. Thanks to Fanny Canesi for her shaping help and insightful comments. This work was supported by the SAM Société des Explorations de Monaco (https://monacoexplorations.org) [grant numbers SAM EDM 01/2019 & 01/2020] and partially by National Science Center (Poland) research grant 2017/25/B/ST10/02221. This is publication number 16 of the Tara Pacific Consortium.

## REFERENCES


Allison, N., Finch, A. A., Webster, J. M., and Clague, D. A., 2007. Palaeoenvironmental records from fossil corals: The effects of submarine diagenesis on temperature and climate estimates. Geochimica et Cosmochimica Acta 71, 4693–4703.

Alpert, A.E., Cohen, A.L., Oppo, D.W., DeCarlo, T.M., Gaetani, G.A., Hernandez-Delgado, E.A., Winter, A., Gonneea, M.E., 2017. Twentieth century warming of the tropical Atlantic captured by Sr-U paleothermometry. Paleoceanography 32, 146–160.

Bagnato, S., Linsley, B., Howe, S., Wellington, G., Salinger, J., 2004. Evaluating the use of the massive coral *Diploastrea heliopora* for paleoclimate reconstruction.

Banzon, V., Smith, T.M., Liu, C., Hankins, W., 2016. A long-term record of blended satellite and in situ sea surface temperature for climate monitoring, modeling and environmental studies. Open Access 13.

Beck, J.W., Edwards, R.L., Ito, E., Taylor, F.W., Recy, J., Rougerie, F., Joannot, P., Henin, C., 1992. Sea-surface temperature from coral skeletal strontium/calcium ratios. Science 257, 644–648.

Bevington, P.R., Robinson, D.K., 1993. Data Reduction and Error Analysis for the Physical Sciences. Computers in Physics 7, 415–416.

Boiseau, M., Juillet-Leclerc, A., Yiou, P., Salvat, B., Isdale, P., Guillaume, M., 1998. Atmospheric and oceanic evidences of El Niño-Southern Oscillation events in the south central Pacific Ocean from coral stable isotopic records over the last 137 years. Paleoceanography 13, 671–685.

Bourdin, C., Douville, E., Genty, D., 2011. Alkaline-earth metal and rare-earth element incorporation control by ionic radius and growth rate on a stalagmite from the Chauvet Cave, Southeastern France. Chemical Geology 290, 1–11.

Bruno, J., Siddon, C., Witman, J., Colin, P., Toscano, M., 2001. El Niño related coral bleaching in Palau, Western Caroline Islands. Coral Reefs 20, 127–136.

Burr, G.S., Beck, J.W., Taylor, F.W., Récy, J., Edwards, R.L., Cabioch, G., Corrège, T., Donahue, D.J., O'Malley, J.M., 1998. A high-resolution radiocarbon calibration between 11,700 and 12,400 calendar years BP derived from $^{230}$Th ages of corals from Espiritu Santo Island, Vanuatu. Radiocarbon 40, 1093–1105.

Case, D.H., Robinson, L.F., Auro, M.E., Gagnon, A.C., 2010. Environmental and biological controls on Mg and Li in deep-sea scleractinian corals. Earth and Planet. Sci. Lett. 300, 215–225.

Cheng, H., Edwards, R.L., Shen, C.C., Polyak, V.J., Asmerom, Y., Woodhead, J., Hellstrom, J., Wang, Y., Kong, X., Spötl, C., Wang, X., Alexander, E.C., 2013. Improvements in $^{230}$Th dating, $^{230}$Th and $^{234}$U half-life values, and U-Th isotopic measurements by multi-collector inductively coupled plasma mass spectrometry. Earth and Planet. Sci. Lett. 371–372, 82–91.

Chutcharavan, P.M., Dutton, A., Ellwood, M.J., 2018. Seawater $^{234}$U/$^{238}$U recorded by modern and fossil corals. Geochimica et Cosmochimica Acta 224, 1–17.

Cocquempot, L., Delacourt, C., Paillet, J., Riou, P., Aucan, J., Castelle, B., Charria, G., Claudet, J., Conan, P., Coppola, L., Hocdé, R., Planes, S., Raimbault, P., Savoye, N., Testut, L., Vuillemin, R., 2019. Coastal Ocean and Nearshore Observation: A French

Case Study. Front. Mar. Sci. 6.
Cohen, A.L., Layne, G.D., Hart, S.R., Lobel, P.S., 2001. Kinetic control of skeletal Sr/Ca in a symbiotic coral: Implications for the paleotemperature proxy. Paleoceanography 16, 20–26.
Cohen, A.L., Owens, K.E., Layne, G.D., Shimizu, N., 2002. The Effect of Algal Symbionts on the Accuracy of Sr/Ca Paleotemperatures from Coral. Science 296, 331–333.
Cole, J.E., Rind, D., Fairbanks, R., 1993. Isotopic responses to interannual climate variability simulated by an atmospheric general circulation model. Quaternary Science Reviews 12, 387–406.
Colin, P.L., 2018. Ocean Warming and the Reefs of Palau. Oceanography 31, 126–135.
Corrège, T., 2006. Sea surface temperature and salinity reconstruction from coral geochemical tracers. Palaeogeography Palaeoclimatology Palaeoecology 232, 408–428.
Corrège, T., Gagan, M.K., Beck, J.W., Burr, G.S., Cabioch, G., Cornec, F.L., 2004. Interdecadal variation in the extent of South Pacific tropical waters during the Younger Dryas event. Nature 428, 927–929.
Cuny-Guirriec, K., Douville, E., Reynaud, S., Allemand, D., Bordier, L., Canesi, M., Mazzoli, C., Taviani, M., Canese, S., McCulloch, M., Trotter, J., Rico-Esenaro, S.D., Sanchez-Cabeza, J.-A., Ruiz-Fernández, A.C., Carricart-Ganivet, J.P., Scott, P.M., Sadekov, A., Montagna, P., 2019. Coral Li/Mg thermometry: Caveats and constraints. Chemical Geology 523, 162–178.
Damassa, T.D., Cole, J.E., Barnett, H.R., Ault, T.R., McClanahan, T.R., 2006. Enhanced multidecadal climate variability in the seventeenth century from coral isotope records in the western Indian Ocean. Paleoceanography 21.
DeCarlo, T.M., 2017. Deriving coral skeletal density from computed tomography (CT): effects of scan and reconstruction settings. Matters Select 3, e201706000005.
DeCarlo, T.M., Gaetani, G.A., Cohen, A.L., Foster, G.L., Alpert, A.E., Stewart, J.A., 2016. Coral Sr-U thermometry. Paleoceanography 31, 626–638.
DeLong, K., M. Quinn, T., Taylor, F., 2007. Reconstructing twentieth-century sea surface temperature variability in the southwest Pacific: A replication study using multiple coral Sr/Ca records from New Caledonia. Paleoceanography 22, PA4212.
DeLong, K.L., Quinn, T.M., Taylor, F.W., Shen, C.-C., Lin, K., 2013. Improving coral-base paleoclimate reconstructions by replicating 350years of coral Sr/Ca variations. Palaeogeography, Palaeoclimatology, Palaeoecology, Unraveling environmental histories from skeletal diaries - advances in sclerochronology 373, 6–24.
DeVantier, L., Turak, E., 2017. Species Richness and Relative Abundance of Reef-Building Corals in the Indo-West Pacific. Diversity 9, 25.
D'Olivo, J.P., Sinclair, D.J., Rankenburg, K., McCulloch, M.T., 2018. A universal multi-trace element calibration for reconstructing sea surface temperatures from long-lived Porites corals: Removing 'vital-effects.' Geochimica et Cosmochimica Acta 239, 109–135.
Douville, E., Sallé, E., Frank, N., Eisele, M., Pons-Branchu, E., Ayrault, S., 2010. Rapid and accurate U–Th dating of ancient carbonates using inductively coupled plasma-quadrupole mass spectrometry. Chemical Geology 272, 1–11.
Dutra, L.X.C., Haywood, M.D.E., Singh, S., Ferreira, M., Johnson, J.E., Veitayaki, J., Kininmonth, S., Morris, C.W., Piovano, S., 2021. Synergies between local and

climate-driven impacts on coral reefs in the Tropical Pacific: A review of issues and adaptation opportunities. Marine Pollution Bulletin 164, 111922.

Englebert, N., Bongaerts, P., Muir, Paul, Hay, K., Hoegh-Guldberg, Ove., 2014. Deepest zooxanthellate corals of the Great Barrier Reef and Coral Sea. Marine Biodiversity 45.

Fallon, S. J., McCulloch, M. T., and Alibert, C., 2003. Examining water temperature proxies in Porites corals from the Great Barrier Reef: a cross-shelf comparison. Coral Reefs 22, 389–404.

Finch, A.A., Allison, N., 2008. Mg structural state in coral aragonite and implications for the paleoenvironmental proxy.

Flannery, J.A., Richey, J.N., Toth, L.T., Kuffner, I.B., Poore, R.Z., 2018. Quantifying Uncertainty in Sr/Ca-Based Estimates of SST From the Coral Orbicella faveolata. Paleoceanography and Paleoclimatology 33, 958–973.

Fowell, S.E., Sandford, K., Stewart, J.A., Castillo, K.D., Ries, J.B., Foster, G.L., 2016. Intrareef variations in Li/Mg and Sr/Ca sea surface temperature proxies in the Caribbean reef-building coral Siderastrea siderea. Paleoceanography 31, 1315–1329.

Frankowiak, K., Wang, X.T., Sigman, D.M., Gothmann, A.M., Kitahara, M.V., Mazur, M., Meibom, A., Stolarski, J., 2016. Photosymbiosis and the expansion of shallow-water corals. Science Advances.

Friedlingstein P., O'sullivan M., Jones M. W., Andrew R. M., Gregor L., Hauck J., Le quéré C., Luijkx I. T., Olsen A., Peters G. P., Peters W., Pongratz J., Schwingshackl C., Sitch S., Canadell J. G., Ciais P., Jackson R. B., Alin S. R., Alkama R., Arneth A., Arora V. K., Bates N. R., Becker M., Bellouin N., Bittig H. C., Bopp L., Chevallier F., Chini L. P., Cronin M., Evans W., Falk S., Feely R. A., Gasser T., Gehlen M., Gkritzalis T., Gloege L., Grassi G., Gruber N., Gürses Ö., Harris I., Hefner M., Houghton R. A., Hurtt G. C., Iida Y., Ilyina T., Jain A. K., Jersild A., Kadono K., Kato E. and Kennedy D. (2022) Global Carbon Budget 2022. *Earth System Science Data* **14**, 4811–4900.

Gaetani, G.A., Cohen, A.L., 2006. Element partitioning during precipitation of aragonite from seawater: A framework for understanding paleoproxies. Geochimica et Cosmochimica Acta 70, 4617–4634.

Gaetani, G.A., Cohen, A.L., Wang, Z., Crusius, J., 2011. Rayleigh-based, multi-element coral thermometry: A biomineralization approach to developing climate proxies. Geochimica et Cosmochimica Acta 75, 1920–1932.

Gagan, M.K., Ayliffe, L.K., Beck, J.W., Cole, J.E., Druffel, E.R.M., Dunbar, R.B., Schrag, D.P., 2000. New views of tropical paleoclimates from corals. Quaternary Science Reviews 19, 45–64.

Gagnon, A.C., Adkins, J.F., Fernandez, D.P., Robinson, L.F., 2007. Sr/Ca and Mg/Ca vital effects correlated with skeletal architecture in a scleractinian deep-sea coral and the role of Rayleigh fractionation. Earth and Planetary Science Letters 261, 280–295.

Goodkin, N.F., Hughen, K.A., Cohen, A.L., 2007. A multicoral calibration method to approximate a universal equation relating Sr/Ca and growth rate to sea surface temperature. Paleoceanography 22.

Goodkin, N.F., Switzer, A.D., McCorry, D., DeVantier, L., True, J.D., Hughen, K.A., Angeline, N., Yang, T.T., 2011. Coral communities of Hong Kong: long-lived corals

in a marginal reef environment. Marine Ecology Progress Series 426, 185–196.
Hathorne, E.C., Felis, T., Suzuki, A., Kawahata, H., Cabioch, G., 2013. Lithium in the aragonite skeletons of massive Porites corals: A new tool to reconstruct tropical sea surface temperatures. Paleoceanography 28, 143–152.
Hendy, E.J., Gagan, M.K., Lough, J.M., McCulloch, M., deMenocal, P.B., 2007. Impact of skeletal dissolution and secondary aragonite on trace element and isotopic climate proxies in *Porites* corals. Paleoceanography 22.
Hoegh-Guldberg, O., 1999. Climate change, coral bleaching and the future of the world's coral reefs. Mar. Freshwater Res. 50, 839–866.
Hoegh-Guldberg, O., Mumby, P.J., Hooten, A.J., Steneck, R.S., Greenfield, P., Gomez, E., Harvell, C.D., Sale, P.F., Edwards, A.J., Caldeira, K., Knowlton, N., Eakin, C.M., Iglesias-Prieto, R., Muthiga, N., Bradbury, R.H., Dubi, A., Hatziolos, M.E., 2007. Coral Reefs Under Rapid Climate Change and Ocean Acidification. Science 318, 1737–1742.
Huang, B., Menne, M. J., Boyer, T., Freeman, E., Gleason, B. E., Lawrimore, J. H., Liu, C., Rennie, J. J., Schreck, C. J., Sun, F., Vose, R., Williams, C. N., Yin, X. and Zhang, H.-M., 2020. Uncertainty Estimates for Sea Surface Temperature and Land Surface Air Temperature in NOAAGlobalTemp Version 5. Journal of Climate 33, 1351–1379.
Hughes, T.P., Kerry, J.T., Álvarez-Noriega, M., Álvarez-Romero, J.G., Anderson, K.D., Baird, A.H., Babcock, R.C., Beger, M., Bellwood, D.R., Berkelmans, R., Bridge, T.C., Butler, I.R., Byrne, M., Cantin, N.E., Comeau, S., Connolly, S.R., Cumming, G.S., Dalton, S.J., Diaz-Pulido, G., Eakin, C.M., Figueira, W.F., Gilmour, J.P., Harrison, H.B., Heron, S.F., Hoey, A.S., Hobbs, J.-P.A., Hoogenboom, M.O., Kennedy, E.V., Kuo, C., Lough, J.M., Lowe, R.J., Liu, G., McCulloch, M.T., Malcolm, H.A., McWilliam, M.J., Pandolfi, J.M., Pears, R.J., Pratchett, M.S., Schoepf, V., Simpson, T., Skirving, W.J., Sommer, B., Torda, G., Wachenfeld, D.R., Willis, B.L., Wilson, S.K., 2017. Global warming and recurrent mass bleaching of corals. Nature 543, 373–377.
Inoue, M., Suwa, R., Suzuki, A., Sakai, K., and Kawahata, H., 2011. Effects of seawater pH on growth and skeletal U/Ca ratios of Acropora digitifera coral polyps. Geophysical Research Letters 38.
Jaffey, A.H., Flynn, K.F., Glendenin, L.E., Bentley, W.C., Essling, A.M., 1971. Precision Measurement of Half-Lives and Specific Activities of $^{235}$U and $^{238}$U. Phys. Rev. C 4, 1889–1906.
Kleypas, J.A., Buddemeier, R.W., Archer, D., Gattuso, J.-P., Langdon, C., Opdyke, B.N., 1999. Geochemical Consequences of Increased Atmospheric Carbon Dioxide on Coral Reefs. Science 284, 118–120.
Knutson, D.W., Buddemeier, R.W., Smith, S.V., 1972. Coral Chronometers: Seasonal Growth Bands in Reef Corals. Science 177, 270–272.
Kroeker, K.J., Kordas, R.L., Crim, R., Hendriks, I.E., Ramajo, L., Singh, G.S., Duarte, C.M., Gattuso, J.-P., 2013. Impacts of ocean acidification on marine organisms: quantifying sensitivities and interaction with warming. Global Change Biology 19, 1884–1896.
Lazareth, C.E., Soares-Pereira, C., Douville, E., Brahmi, C., Dissard, D., Le Cornec, F., Thil, F., Gonzalez-Roubaud, C., Caquineau, S., Cabioch, G., 2016. Intra-skeletal calcite in a

live-collected Porites sp.: Impact on environmental proxies and potential formation process. Geochimica et Cosmochimica Acta 176, 279–294.
Linsley, B.K., Messier, R.G., Dunbar, R.B., 1999. Assessing between-colony oxygen isotope variability in the coral Porites lobata at Clipperton Atoll. Coral Reefs 18, 13–27.
Locarnini, M., Mishonov, A., Baranova, O., Boyer, T., Zweng, M., Garcia, H., Reagan, J., Seidov, D., Weathers, K., Paver, C., Smolyar, I., 2018. World Ocean Atlas 2018, Volume 1: Temperature.
López-Correa, M., Montagna, P., Vendrell-Simón, B., McCulloch, M., Taviani, M., 2010. Stable isotopes ($\delta^{18}O$ and $\delta^{13}C$), trace and minor element compositions of Recent scleractinians and Last Glacial bivalves at the Santa Maria di Leuca deep-water coral province, Ionian Sea. Deep Sea Research Part II: Topical Studies in Oceanography 57, 471–486.
Lough, J.M., 2010. Climate records from corals. WIREs Climate Change 1, 318–331.
Lough, J.M., 2008. Coral calcification from skeletal records revisited. Marine Ecology Progress Series 373, 257–264.
Lough, J.M., Barnes, D.J., 1992. Comparisons of skeletal density variations in Porites from the central Great Barrier Reef. Journal of Experimental Marine Biology and Ecology 155, 1–25.
Ludwig, K.R., Titterington, D.M., 1994. Calculation of 230Th /U isochrons, ages, and errors. Geochimica et Cosmochimica Acta 58, 5031–5042.
Macintyre, I.G., Towe, K.M., 1976. Skeletal Calcite in Living Scleractinian Corals: Microboring Fillings, Not Primary Skeletal Deposits. Science.
Marchitto, T.M., Bryan, S.P., Doss, W., McCulloch, M.T., Montagna, P., 2018. A simple biomineralization model to explain Li, Mg, and Sr incorporation into aragonitic foraminifera and corals. Earth and Planetary Science Letters 481, 20–29.
Marriott, C.S., Henderson, G.M., Crompton, R., Staubwasser, M., Shaw, S., 2004. Effect of mineralogy, salinity, and temperature on Li/Ca and Li isotope composition of calcium carbonate. Chemical Geology, Lithium Isotope Geochemistry 212, 5–15.
McGregor, H.V., Gagan, M.K., 2003. Diagenesis and geochemistry of porites corals from Papua New Guinea: Implications for paleoclimate reconstruction. Geochimica et Cosmochimica Acta 67, 2147–2156.
Meibom, A., Cuif, J.-P., Hillion, F., Constantz, B.R., Juillet-Leclerc, A., Dauphin, Y., Watanabe, T., Dunbar, R.B., 2004. Distribution of magnesium in coral skeleton. Geophysical Research Letters 31.
Meibom, A., Yurimoto, H., Cuif, J.-P., Domart-Coulon, I., Houlbrèque, F., Constantz, B., Dauphin, Y., Tambutté, E., Tambutté, S., Allemand, D., Wooden, J., Dunbar, R., 2006. Vital effects in coral skeleton display strict three-dimensional control. Geophys. Res. Lett. 33, L11608.
Mitsuguchi, T., Matsumoto, E., Abe, O., Uchida, T., Isdale, P.J., 1996. Mg/Ca Thermometry in Coral Skeletons. Science 274, 961–963.
Montagna, P., McCulloch, M., Douville, E., Correa, M.L., Trotter, J., Rodolfo-Metalpa, R., Dissard, D., Ferrier-Pagès, C., Frank, N., Freiwald, A., Goldstein, S.L., Mazzoli, C., Reynaud, S., Rüggeberg, A., Russo, S., Taviani, M., 2014. Li/Mg systematics in scleractinian corals: Calibration of the thermometer. Geochimica et Cosmochimica

Acta 132, 288–310.
Montagna, P., McCulloch, M., Mazzoli, C., and Silenzi, S., 2007. The non-tropical coral Cladocora caespitosa as the new climate archive for the Mediterranean: high-resolution (~weekly) trace element systematics. Quaternary Science Reviews 26, 441–462.
Montagna, P., McCulloch, M., Taviani, M., Remia, A., Rouse, G., 2005. High-resolution trace and minor element compositions in deep-water scleractinian corals (Desmophyllum dianthus) from the Mediterranean Sea and the Great Australian Bight, in: Freiwald, A., Roberts, J.M. (Eds.), Cold-Water Corals and Ecosystems, Erlangen Earth Conference Series. Springer, Berlin, Heidelberg, pp. 1109–1126.
Nothdurft, L.D., Webb, G.E., 2009. Earliest diagenesis in scleractinian coral skeletons: implications for palaeoclimate-sensitive geochemical archives. Facies 55, 161–201.
Okai, T., Suzuki, A., Kawahata, H., Terashima, S., Imai, N., 2002. Preparation of a New Geological Survey of Japan Geochemical Reference Material: Coral JCp-1. Geostandards Newsletter 26, 95–99.
Osborne, M.C., Dunbar, R.B., Mucciarone, D.A., Sanchez-Cabeza, J.-A., Druffel, E., 2013. Regional calibration of coral-based climate reconstructions from Palau, West Pacific Warm Pool (WPWP). Palaeogeography, Palaeoclimatology, Palaeoecology 386, 308–320.
Pfeiffer, M., Dullo, W.-C., Zinke, J., Garbe-Schönberg, D., 2009. Three monthly coral Sr/Ca records from the Chagos Archipelago covering the period of 1950–1995 A.D.: reproducibility and implications for quantitative reconstructions of sea surface temperature variations. Int J Earth Sci (Geol Rundsch) 98, 53–66.
Pfeiffer, M., Zinke, J., Dullo, W.-C., Garbe-Schönberg, D., Latif, M., Weber, M.E., 2017. Indian Ocean corals reveal crucial role of World War II bias for twentieth century warming estimates. Scientific Reports 7, 14434.
Planes, S., Allemand, D., Agostini, S., Banaigs, B., Boissin, E., Boss, E., Bourdin, G., Bowler, C., Douville, E., Flores, J.M., Forcioli, D., Furla, P., Galand, P.E., Ghiglione, J.-F., Gilson, E., Lombard, F., Moulin, C., Pesant, S., Poulain, J., Reynaud, S., Romac, S., Sullivan, M.B., Sunagawa, S., Thomas, O.P., Troublé, R., de Vargas, C., Vega Thurber, R., Voolstra, C.R., Wincker, P., Zoccola, D., Tara Pacific Consortium, 2019. The Tara Pacific expedition-A pan-ecosystemic approach of the "-omics" complexity of coral reef holobionts across the Pacific Ocean. PLoS Biol 17, e3000483.
Pons-Branchu, E., Douville, E., Roy-Barman, M., Dumont, E., Branchu, P., Thil, F., Frank, N., Bordier, L., Borst, W., 2014. A geochemical perspective on Parisian urban history based on U–Th dating, laminae counting and yttrium and REE concentrations of recent carbonates in underground aqueducts. Quaternary Geochronology 24, 44–53.
Quinn, T.M., Crowley, T., Taylor, F.W., Hénin, C., Joannot, P., Join, Y., 1998. A multicentury stable isotope record from a New Caledonia coral: Interannual and decadal sea surface temperature variability in the southwest Pacific since 1657 A.D.
Quinn, T.M., Sampson, D.E., 2002. A multiproxy approach to reconstructing sea surface conditions using coral skeleton geochemistry. Paleoceanography 17, 1062.
Ram, S. and Erez, J., 2021. The Distribution Coefficients of Major and Minor Elements in Coral Skeletons Under Variable Calcium Seawater Concentrations. Frontiers in Earth

Science 9, 336.
Ram, S., and Erez, J., 2023. Anion elements incorporation into corals skeletons: Experimental approach for biomineralization and paleo-proxies. Proceedings of the National Academy of Sciences 120, e2306627120.
Ramos, R.D., Goodkin, N.F., Siringan, F.P., Hughen, K.A., 2017. Diploastrea heliopora Sr/Ca and δ18O records from northeast Luzon, Philippines: An assessment of interspecies coral proxy calibrations and climate controls of sea surface temperature and salinity. Paleoceanography 32, 424–438.
Rayner, N.A., Parker, D.E., Horton, E.B., Folland, C.K., Alexander, L.V., Rowell, D.P., Kent, E.C., Kaplan, A., 2003. Global analyses of sea surface temperature, sea ice, and night marine air temperature since the late Nineteenth Century. Journal of Geophysical Research 108, 4407-[37pp].
Reynolds, R.W., Smith, T.M., Liu, C., Chelton, D.B., Casey, K.S., Schlax, M.G., 2007. Daily High-Resolution-Blended Analyses for Sea Surface Temperature. J. Climate 20, 5473–5496.
Ross, C.L., DeCarlo, T.M., McCulloch, M.T., 2019. Environmental and physiochemical controls on coral calcification along a latitudinal temperature gradient in Western Australia. Global Change Biology 25, 431–447.
Saenger, C., Cohen, A.L., Oppo, D.W., Hubbard, D., 2008. Interpreting sea surface temperature from strontium/calcium ratios in *Montastrea* corals: Link with growth rate and implications for proxy reconstructions. Paleoceanography 23.
Sayani, H.R., Cobb, K.M., Cohen, A.L., Elliott, W.C., Nurhati, I.S., Dunbar, R.B., Rose, K.A., Zaunbrecher, L.K., 2011. Effects of diagenesis on paleoclimate reconstructions from modern and young fossil corals. Geochimica et Cosmochimica Acta 75, 6361–6373.
Shen, G. T., and Dunbar, R., 1995. Environmental controls on uranium in reef corals.
Sinclair, D.J., 2015. RBME coral temperature reconstruction: An evaluation, modifications, and recommendations. Geochimica et Cosmochimica Acta 154, 66–80.
Sinclair, D.J., Kinsley, L.P.J., McCulloch, M.T., 1998. High resolution analysis of trace elements in corals by laser ablation ICP-MS. Geochimica et Cosmochimica Acta 62, 1889–1901.
Sinclair, D.J., Risk, M.J., 2006. A numerical model of trace-element coprecipitation in a physicochemical calcification system: Application to coral biomineralization and trace-element 'vital effects.' Geochimica et Cosmochimica Acta 70, 3855–3868.
Solow, A., Huppert, A., 2004. Optimal multiproxy reconstruction of sea surface temperature from corals. Paleoceanography 19.
Stocker, T.F., Qin, D., Plattner, G.-K., Tignor, M., Allen, S.K., Boschung, J., Nauels, A., Xia, Y., Bex, V., Midgley, P.M., 2013. Climate change 2013: The physical science basis. Contribution of working group I to the fifth assessment report of the intergovernmental panel on climate change 1535.
Stolarski, J., 2003. Three-dimensional micro- and nanostructural characteristics of the scleractinian coral skeleton: A biocalcification proxy. Acta Palaeontologica Polonica 48.
Stolarski, J., Kitahara, M.V., Miller, D.J., Cairns, S.D., Mazur, M., Meibom, A., 2011. The

ancient evolutionary origins of Scleractinia revealed by azooxanthellate corals. BMC Evolutionary Biology 11, 316.
Stolarski, J., Coronado, I., Murphy, J.G., Kitahara, M.V., Janiszewska, K., Mazur, M., et al., 2021. A modern scleractinian coral with a two-component calcite–aragonite skeleton. Proc. Natl. Acad. Sci. 118, e2013316117.
Tangri, N., Dunbar, R.B., Linsley, B.K., Mucciarone, D.M., 2018. ENSO's Shrinking Twentieth-Century Footprint Revealed in a Half-Millennium Coral Core From the South Pacific Convergence Zone. Paleoceanography and Paleoclimatology 33, 1136–1150.
Tierney, J.E., Abram, N.J., Anchukaitis, K.J., Evans, M.N., Giry, C., Kilbourne, K.H., Saenger, C.P., Wu, H.C., Zinke, J., 2015. Tropical sea surface temperatures for the past four centuries reconstructed from coral archives. Paleoceanography 30, 226–252.
Urban, F.E., Cole, J.E., Overpeck, J.T., 2000. Influence of mean climate change on climate variability from a 155-year tropical Pacific coral record. Nature 407, 989–993.
van Woesik, R., Golbuu, Y., Roff, G., 2015. Keep up or drown: adjustment of western Pacific coral reefs to sea-level rise in the 21st century. Royal Society Open Science 2, 150181.
van Woesik, R. van, Houk, P., Isechal, A.L., Idechong, J.W., Victor, S., Golbuu, Y., 2012. Climate-change refugia in the sheltered bays of Palau: analogs of future reefs. Ecology and Evolution 2, 2474–2484.
Varillon, D., Fiat, S., Magron, F., Allenbach, M., Hoibian, T., De Ramon N'Yeurt, A., Ganachaud, A., Aucan, J., Pelletier, B., Hocdé, R., 2019. ReefTEMPS : The Pacific Island coastal ocean observation network.
Wang, H., Mehta, V.M., 2008. Decadal Variability of the Indo-Pacific Warm Pool and Its Association with Atmospheric and Oceanic Variability in the NCEP–NCAR and SODA Reanalyses. J. Climate 21, 5545–5565.
Watanabe, T., Gagan, M.K., Corrége, T., Scott-Gagan, H., Cowley, J., Hantoro, W.S., 2003a. Oxygen isotope systematics in Diploastrea heliopora: new coral archive of tropical paleoclimate. Geochimica et Cosmochimica Acta 67, 1349–1358.
Weber, J.N., Woodhead, P.M.J., 1972. Temperature dependence of oxygen-18 concentration in reef coral carbonates. Journal of Geophysical Research (1896-1977) 77, 463–473.
Wei, G., Sun, M., Li, X., and Nie, B., 2000. Mg/Ca, Sr/Ca and U/Ca ratios of a porites coral from Sanya Bay, Hainan Island, South China Sea and their relationships to sea surface temperature. Palaeogeography, Palaeoclimatology, Palaeoecology 162, 59–74.
Wu, H.C., Dissard, D., Douville, E., Blamart, D., Bordier, L., Tribollet, A., Le Cornec, F., Pons-Branchu, E., Dapoigny, A., Lazareth, C.E., 2018. Surface ocean pH variations since 1689 CE and recent ocean acidification in the tropical South Pacific. Nature Communications 9, 2543.
Wu, Y., Fallon, S.J., Cantin, N.E., Lough, J.M., 2021. Assessing multiproxy approaches (Sr/Ca, U/Ca, Li/Mg, and B/Mg) to reconstruct sea surface temperature from coral skeletons throughout the Great Barrier Reef. Science of The Total Environment 786, 147393.
Zinke, J., d'Olivo, J., Gey, C., Mcculloch, M., Bruggemann, J.H., Lough, J., Guillaume, M.M.M., 2019. Multi-trace-element sea surface temperature coral reconstruction for the southern Mozambique Channel reveals teleconnections with the tropical Atlantic.

Biogeosciences 16, 695–712.
Zinke, J., Rountrey, A., Feng, M., Xie, S.-P., Dissard, D., Rankenburg, K., Lough, J.M., McCulloch, M.T., 2014. Corals record long-term Leeuwin current variability including Ningaloo Niño/Niña since 1795. Nature Communications 5, 3607.

**Figure captions**

Fig. 1. Map of the Pacific Ocean showing the sampling locations of coral cores collected during the TARA-Pacific expedition and used to generate SST-calibrations (light blue dots). The mean SST (°C) was obtained from AVHRR-OISSTv2 for the period 2010-2016.

Fig. 2. Map of the Palau archipelago showing the location of the I26S1 site (red circle) where *Porites* and *Diploastrea* colonies were drilled, and Ebiil Channel site (red diamond) where *in-situ* SST were collected.

Fig. 3. Image and X-ray computed tomography scan of *Porites* core-top coral collected in Fiji in June 2017. Light (dark) bands indicate relatively high (low) skeletal density. Timescale is derived from annual density banding counting. Black and white lines represent the sampling transect for geochemical analyses along the main growth axis, corresponding to the last six years of growth (2010-2016).

Fig. 4. X-ray negative radiographs of 8 mm slices of *Porites* (top) and *Diploastrea* (bottom) cores collected in Palau, showing the annual density banding pattern. White lines mark the sampling transects for geochemical analyses along the main growth axes. White dots and diamonds mark the samples analyzed for U/Th dating and XRD characterization, respectively.

Fig. 5. Preservation of examined specimens of *Porites* sp. (A-C, G-I) SEM images of broken longitudinal sections of corallites showing thin dissepiments (examples with black arrow) and pores between septa and columella which are not covered or infilled with any secondary deposits. (D-F, J-L) SEM images of transverse delicately etched sections of septa with hollowed-up regions of microcrystalline Rapid Accretion Deposits (RAD's) (white arrows) and Thickening Deposits often with regular growth increments, typical of zooxanthellate corals (e.g., J, K). Only exceptionally some microboring traces are detectable (dashed red circles, D, L). Specimens: (A,D) I5S4-P_core top (R-SCL-1147); (B, E) I31S3-P_core top (R-SCL-1148); (C, F) I26S1_075_076_077 (R-SCL-1149); (G, J) I253c21-P_core top (R-SCL-1150); (H, K) I32S1-P (R-SCL-1151); (I, L) I26S1_068_067_066 (R-SCL-1152).

Fig. 6. Pristine preservation of examined specimens of *Diploastrea heliopora*. (A-E) SEM images of broken longitudinal sections of corallites showing thin dissepiments (example with arrow) and pores between septa and columella which are not covered or infilled with secondary deposits. (F-J) SEM images of transverse delicately etched sections of septa to show hollowed-up regions of microcrystalline Rapid Accretion Deposits (RAD's) (arrows) and Thickening Deposits often with

regular growth increments, typical of zooxanthellate corals (e.g. F, G). Only exceptionally some microboring traces are detectable (dashed red circles, F, I). Specimens: (A, F) I26S1_322-324 (R-SCL-1153); (B, G) I26S1_208-210 (R-SCL-1154); (C, H) I26S1_004-006 (R-SCL-1155); (D, I) I24S2_c3-D (R-SCL-1156); (E, J) I26S1D_293-295 (R-SCL-1157).

Fig. 7. Robust regressions of (A) Sr/Ca, (B) Li/Mg, and (C) Sr-U for *Porites* (n=34, blue circle) and *Diploastrea* (n=6, red circle) using AVHRR-OISSTv2. In figures 7A and 7B, the dotted and solid lines represent regression lines from the literature and this study, respectively. The Y-errors account for the analytical and the intra-colonial uncertainties and were calculated by adding the errors in quadrature. In Fig. 7C, Sr-U values from this study are combined with those from the literature (DeCarlo et al., 2016; Alpert et al., 2017; Ross et al., 2019). Coloured circles with black dots denote samples with percentage of calcite higher than the detection limit (DL = 0.6 %).

Fig. 8. Reconstructed SST (°C) from *Porites* (I5S4, I21S2c16, I22S2c2) and *Diploastrea* (I21S2c17) core-tops sampled in triplicate. The derived-SST are calculated using the multi-genera SST-calibrations (Eq. B, C, D, E, G for both genera). For the *Porites* colonies, the SST values derived from *Porites*-specific and multi-genera SST calibrations are indistinguishable. As the *Diploastrea*-specific calibrations are less robust, the data are not shown. Grey bands denote the seawater temperature at the sampling location based on AVHRR-OISSTv2 dataset.

Fig. 9. Comparison of mean reconstructed SST in Palau from *Porites* and *Diploastrea* colonies based on single- and multi-ratio calibration equations developed in this study and SST from the AVHRR-OISSTv2 dataset (Reynolds et al., 2007) over the 1982-2016 period. Green boxplots (Eq. D, E, and G) indicate that coral-based mean SST values are not significantly different from OISST (one-way ANOVA test).

Fig. 10. Sub-annual SST changes from 1982 to 2016 in Palau based on *Porites* (A, C) and *Diploastrea* (B, D) colonies compared to OiSSTv2 changes (black line). Coral-based SST records are calculated using (A, B) multi-genera, (C) *Porites*-specific, *Diploastrea*-specific calibration equations developed in this study.

Fig. 11. Relative share (ratio) of two main microstructural components i.e., Rapid Accretion Deposits (RAD's) vs. Thickening Deposits (TD's) in skeleton of *Porites*. Left column shows etched skeletal sections with hollow-out regions representing RAD's surrounded by TD's; middle column shows outlines of RAD's that correspond to hollowed-out regions in the let column; right column shows relationship between RAD's and TD's. RAD's/TD's ratio in *Porites* varies between 6 and 11 % of the bulk skeleton. Relative enrichment of the skeleton of this taxon in elements such as Mg, Li and Ba can

1234 be linked with higher growth dynamics at microscale (and higher relative abundance of RAD's vs.
1235 TD's).
1236 Fig. 12. Relative share (ratio) of two main microstructural components i.e., Rapid Accretion Deposits
1237 (RAD's) vs. Thickening Deposits (TD's) in skeleton of *Diploastrea*. Left column shows etched
1238 skeletal sections with hollow-out regions representing RAD's surrounded by TD's; middle column
1239 shows outlines of RAD's that correspond to hollowed-out regions in the let column; right column
1240 shows relationship between RAD's and TD's. RAD's/TD's ratio in *Diploastrea* varies between 1.2 and
1241 1.8 % of the bulk skeleton. Lower proportion of RAD's vs TD's in the skeleton of this taxon in
1242 comparison to *Porites* suggests relative depletion of elements such as Mg, Li and Ba whose higher
1243 concentrations are linked with faster growing skeletal regions.
1244
1245 Fig. 13. SST records in Palau reconstructed from the *Diploastrea* colony over the period 1874-2016,
1246 expressed as anomalies relative to the 1961-1990 period. Coral-based records are calculated using
1247 multi-genera SST-calibrations of this study and compared to the ERSSTv5 time series. (A) ERSST,
1248 (B) Sr/Ca (Eq. B), (C) Sr-U (Eq. G), (D) Li/Mg (Eq. C), (E) Sr/Ca-Li/Mg (Eq. D) and (F) Sr/Ca-
1249 Li/Ca-Mg/Ca-SST (Eq. E). Black dotted lines correspond to SST trends over the 1874-2016 period.
1250 Black curves correspond to the 5-year average SST.

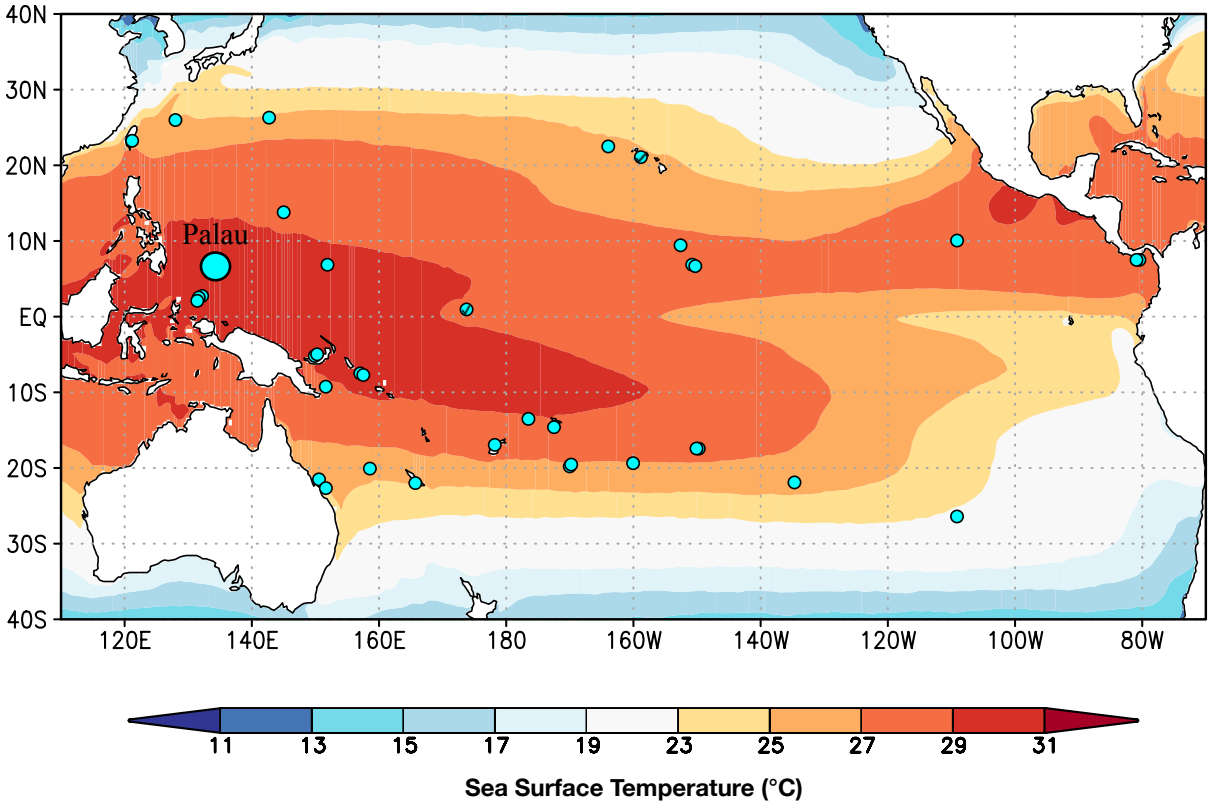
40N
30N
20N
10N
EQ
10S
20S
30S
40S
120E
140E
160E
180
160W
140W
120W
100W
80W
Palau
11
13
15
17
19
23
25
27
29
31
Sea Surface Temperature (°C)

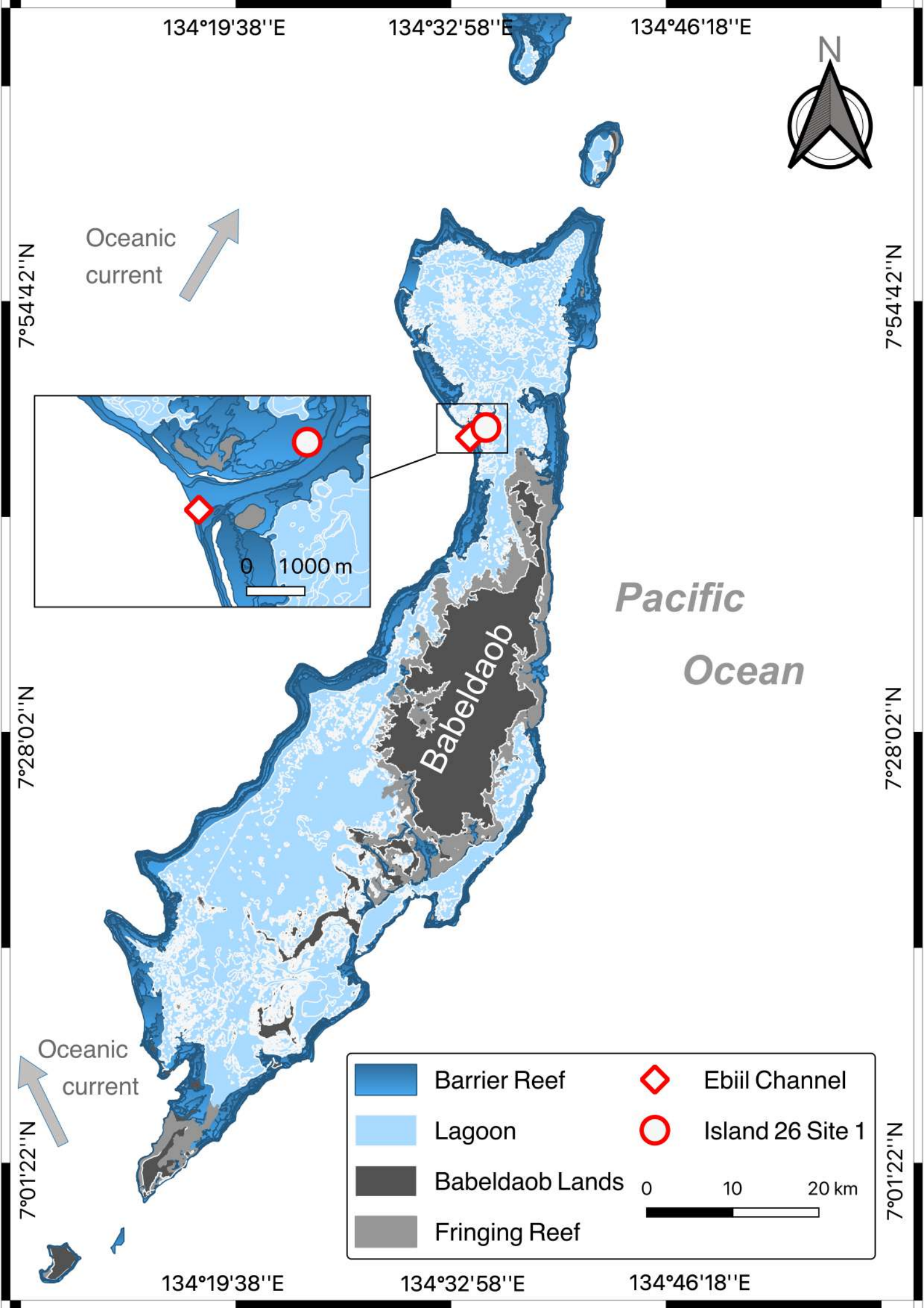
134°19'38''E
134°32'58''E
134°46'18''E
N
7°54'42''N
7°28'02''N
7°01'22''N
Oceanic current
Oceanic current
0 1000 m
Babeldaob
Pacific Ocean
Barrier Reef
Lagoon
Babeldaob Lands
Fringing Reef
Ebiil Channel
Island 26 Site 1
0 10 20 km

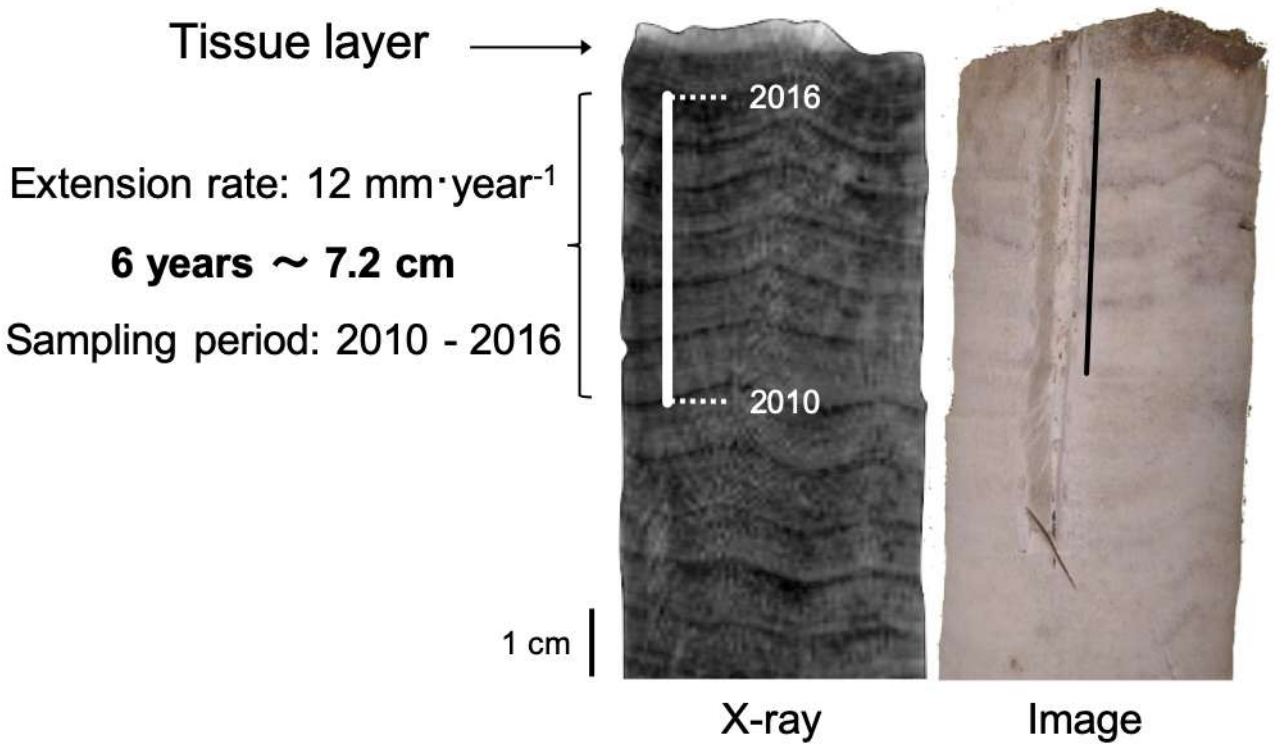
Tissue layer
Extension rate: 12 mm·year-1
6 years ~ 7.2 cm
Sampling period: 2010 - 2016
2016
2010
1 cm
X-ray
Image

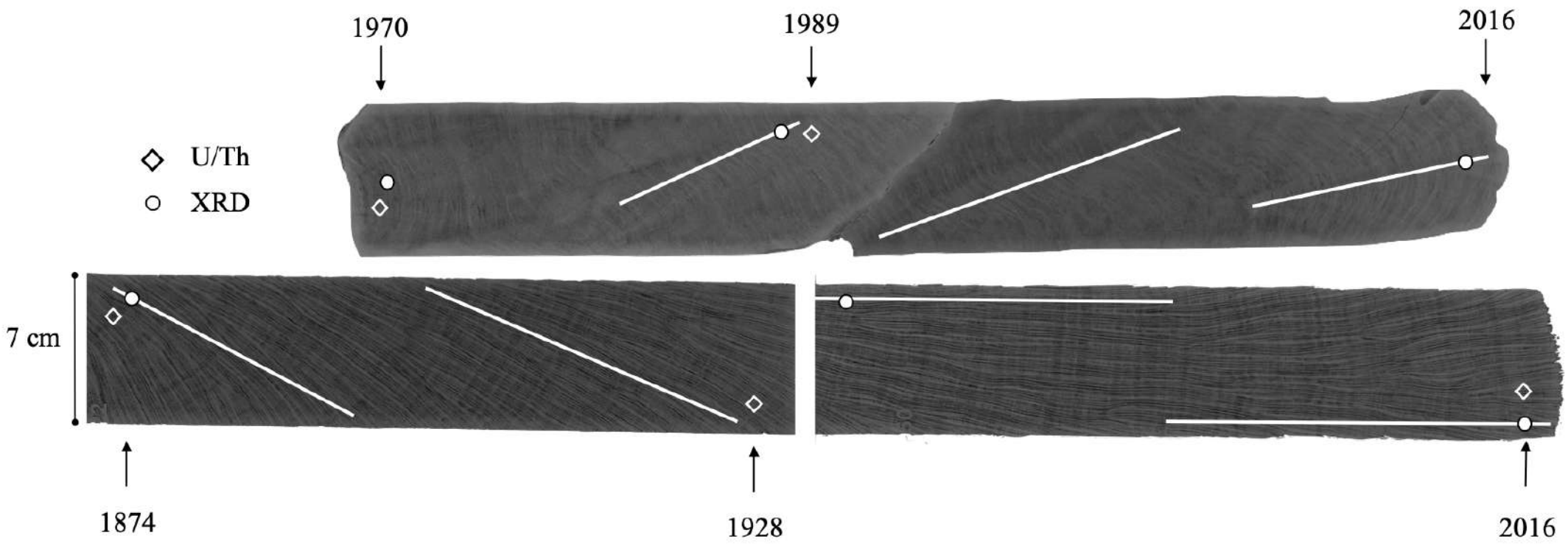
1970
1989
2016
U/Th
XRD
7 cm
1874
1928
2016

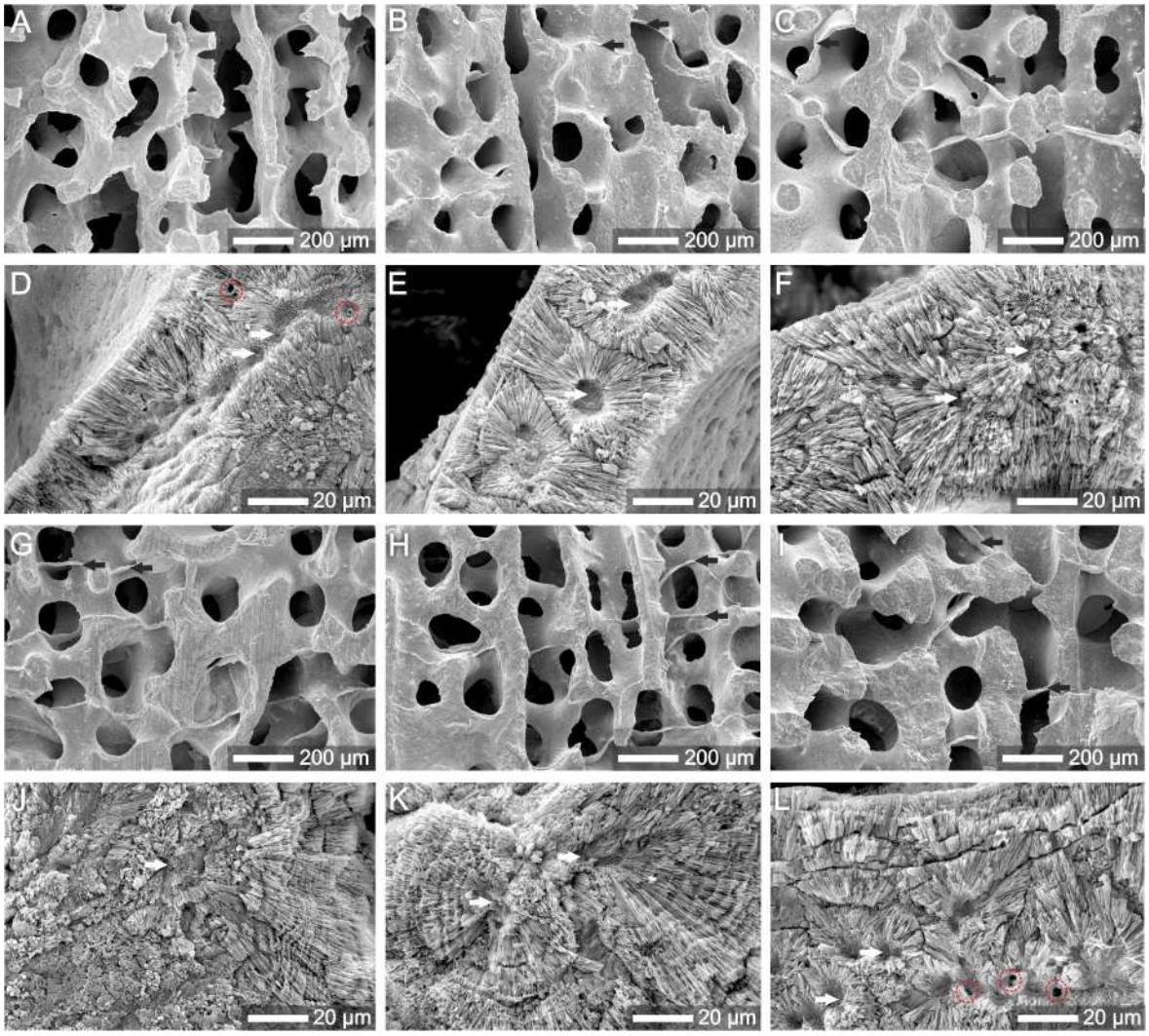
A
200 µm
B
200 µm
C
200 µm
D
20 µm
E
20 µm
F
20 µm
G
200 µm
H
200 µm
I
200 µm
J
20 µm
K
20 µm
L
20 µm

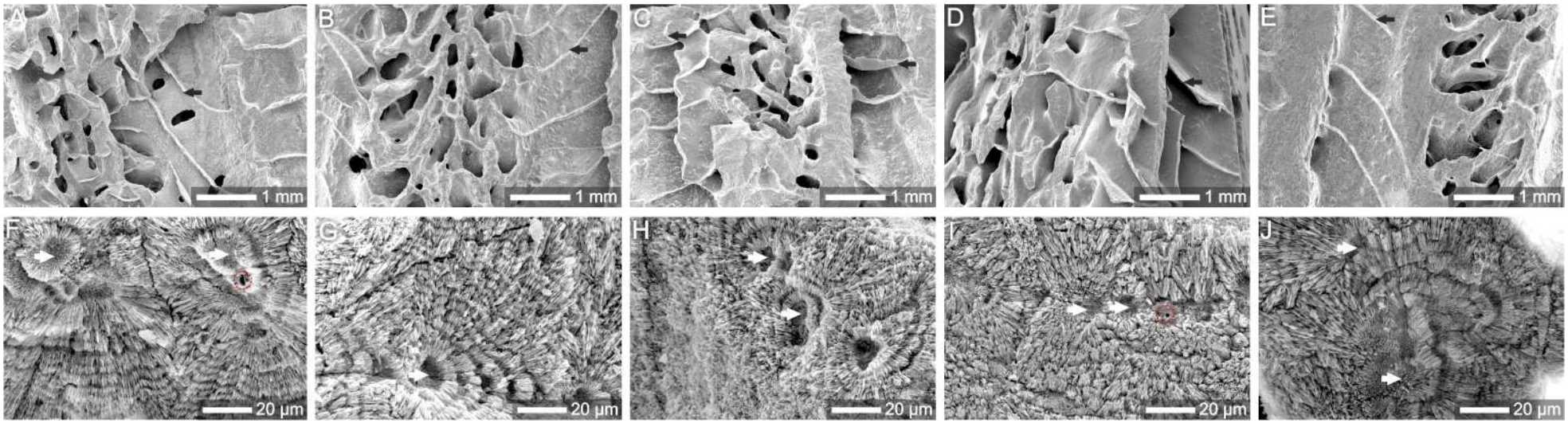
A
1 mm
B
1 mm
C
1 mm
D
1 mm
E
1 mm
F
20 µm
G
20 µm
H
20 µm
I
20 µm
J
20 µm

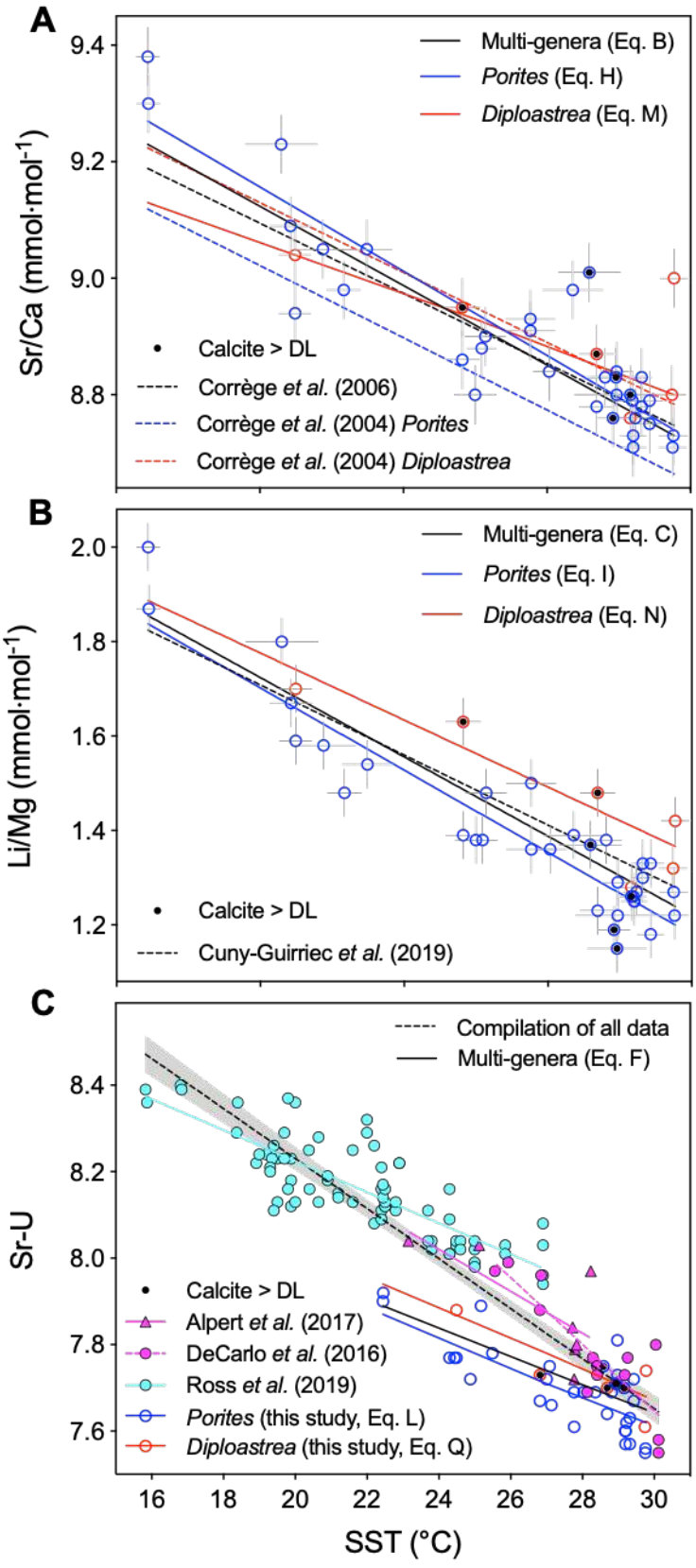
A
Sr/Ca (mmol·mol-1)
9.4
9.2
9.0
8.8
Multi-genera (Eq. B)
Porites (Eq. H)
Diploastrea (Eq. M)
Calcite > DL
Corrège et al. (2006)
Corrège et al. (2004) Porites
Corrège et al. (2004) Diploastrea
B
Li/Mg (mmol·mol-1)
2.0
1.8
1.6
1.4
1.2
Multi-genera (Eq. C)
Porites (Eq. I)
Diploastrea (Eq. N)
Calcite > DL
Cuny-Guirriec et al. (2019)
C
Sr-U
8.4
8.2
8.0
7.8
7.6
Compilation of all data
Multi-genera (Eq. F)
Calcite > DL
Alpert et al. (2017)
DeCarlo et al. (2016)
Ross et al. (2019)
Porites (this study, Eq. L)
Diploastrea (this study, Eq. Q)
16
18
20
22
24
26
28
30
SST (°C)

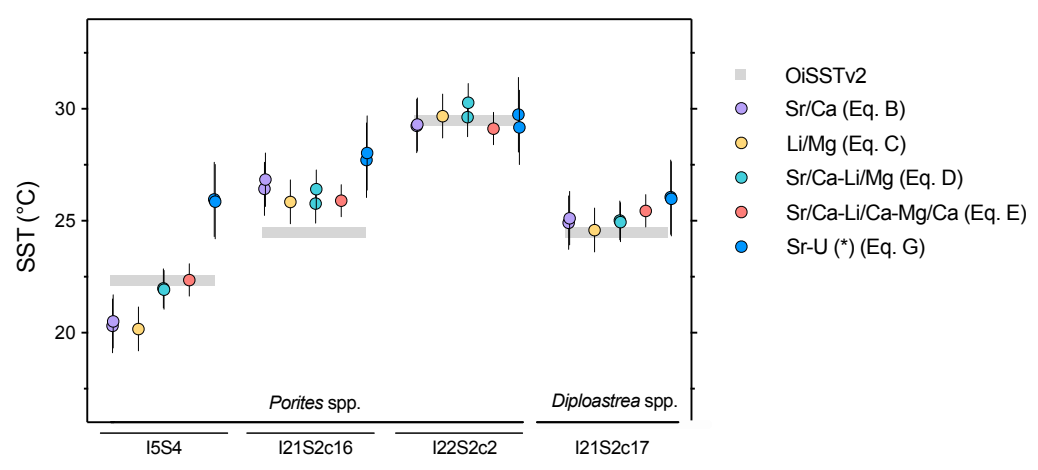
SST (°C)
30
25
20
Porites spp.
Diploastrea spp.
I5S4
I21S2c16
I22S2c2
I21S2c17
OiSSTv2
Sr/Ca (Eq. B)
Li/Mg (Eq. C)
Sr/Ca-Li/Mg (Eq. D)
Sr/Ca-Li/Ca-Mg/Ca (Eq. E)
Sr-U (*) (Eq. G)

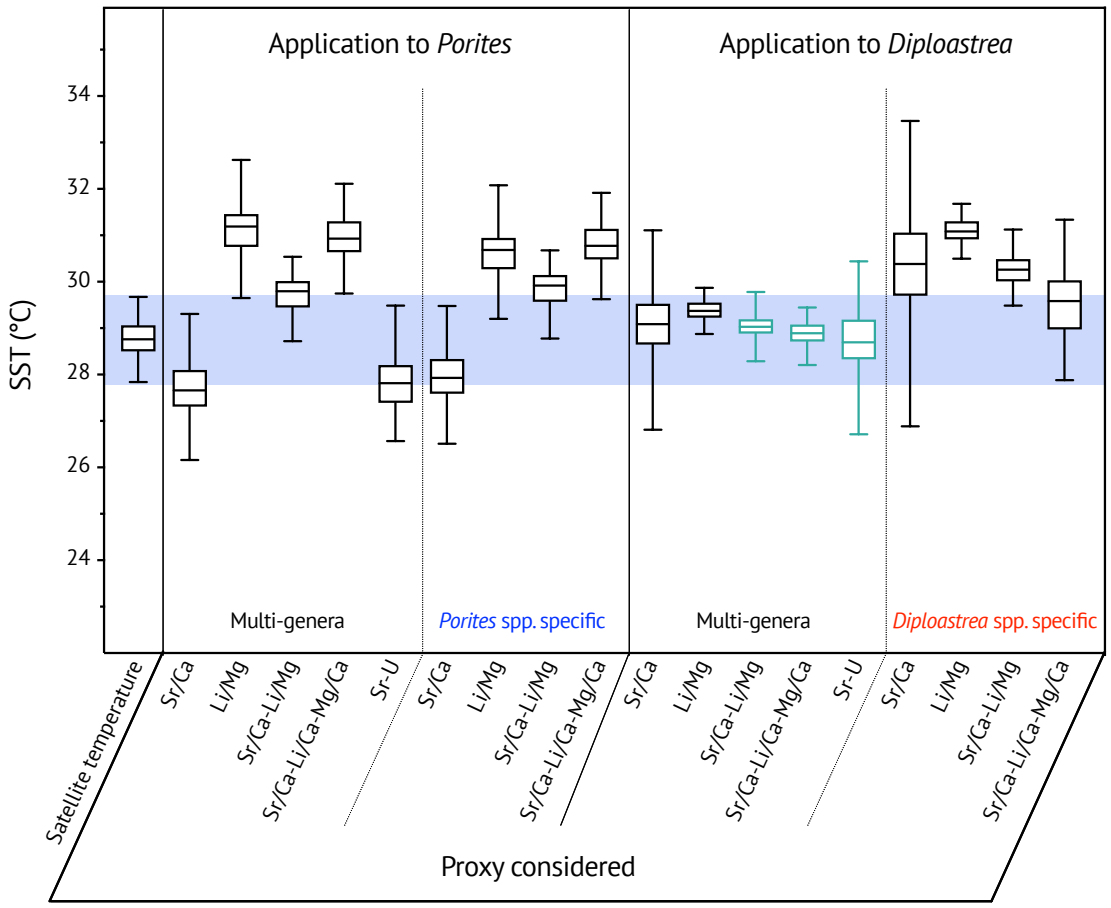
Application to *Porites*
Application to *Diploastrea*
SST (°C)
34
32
30
28
26
24
Multi-genera
*Porites* spp. specific
Multi-genera
*Diploastrea* spp. specific
Satellite temperature
Sr/Ca
Li/Mg
Sr/Ca-Li/Mg
Sr/Ca-Li/Ca-Mg/Ca
Sr-U
Sr/Ca
Li/Mg
Sr/Ca-Li/Mg
Sr/Ca-Li/Ca-Mg/Ca
Sr/Ca
Li/Mg
Sr/Ca-Li/Mg
Sr/Ca-Li/Ca-Mg/Ca
Sr-U
Sr/Ca
Li/Mg
Sr/Ca-Li/Mg
Sr/Ca-Li/Ca-Mg/Ca
Proxy considered

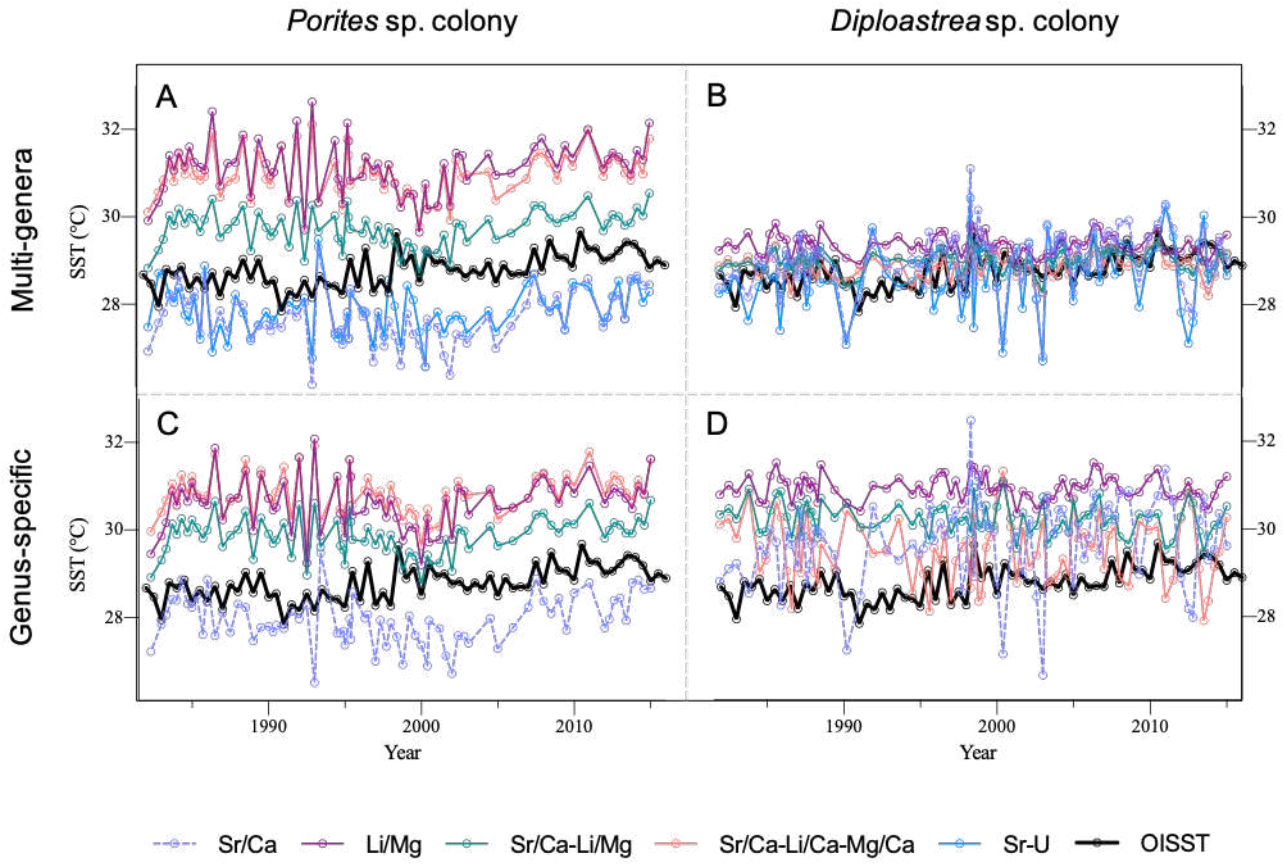
*Porites* sp. colony
*Diploastrea* sp. colony
Multi-genera
Genus-specific
A
B
C
D
SST (°C)
32
30
28
1990
2000
2010
Year
Sr/Ca
Li/Mg
Sr/Ca-Li/Mg
Sr/Ca-Li/Ca-Mg/Ca
Sr-U
OISST

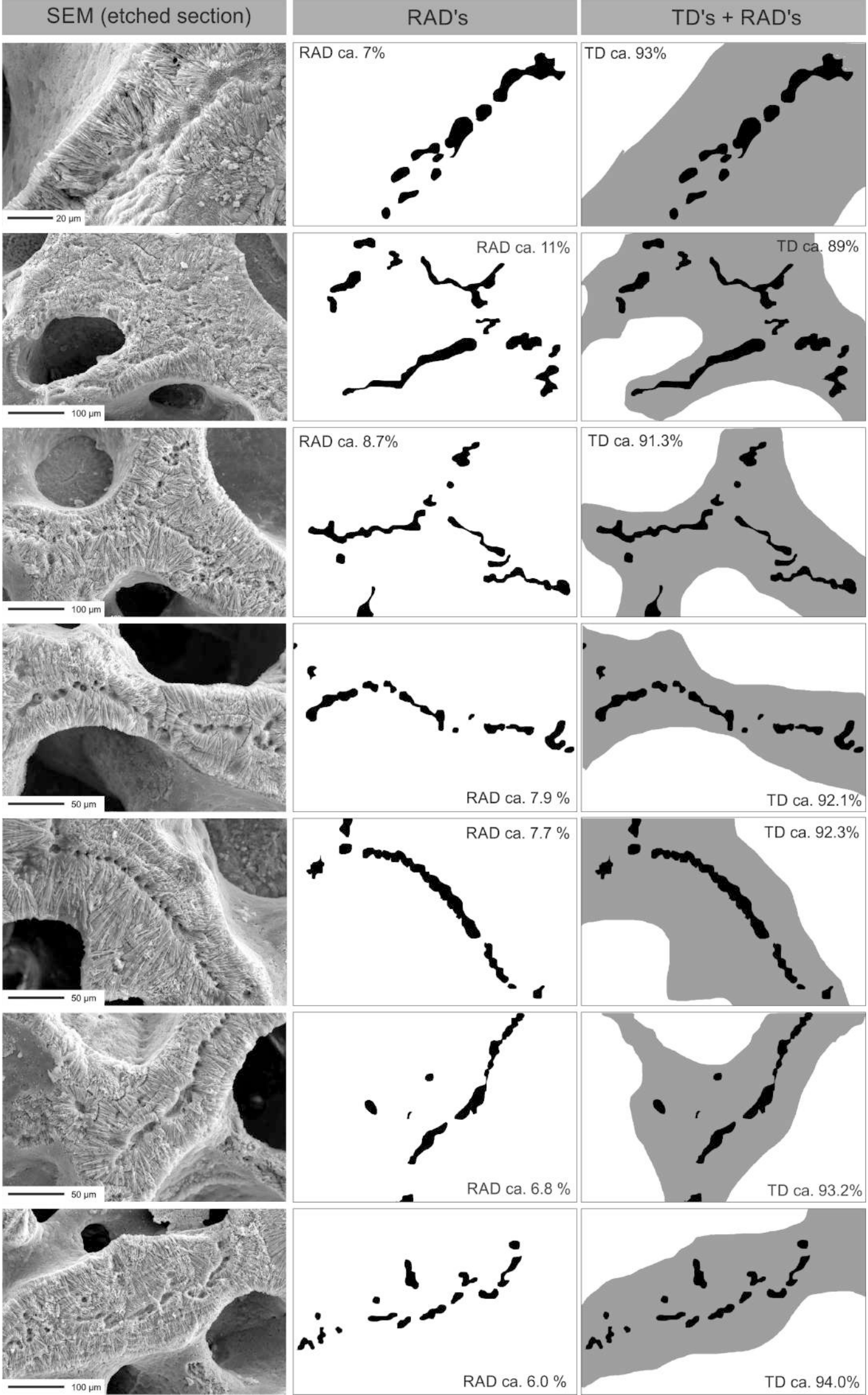
SEM (etched section)
RAD's
TD's + RAD's
RAD ca. 7%
TD ca. 93%
20 µm
RAD ca. 11%
TD ca. 89%
100 µm
RAD ca. 8.7%
TD ca. 91.3%
100 µm
RAD ca. 7.9 %
TD ca. 92.1%
50 µm
RAD ca. 7.7 %
TD ca. 92.3%
50 µm
RAD ca. 6.8 %
TD ca. 93.2%
50 µm
RAD ca. 6.0 %
TD ca. 94.0%
100 µm

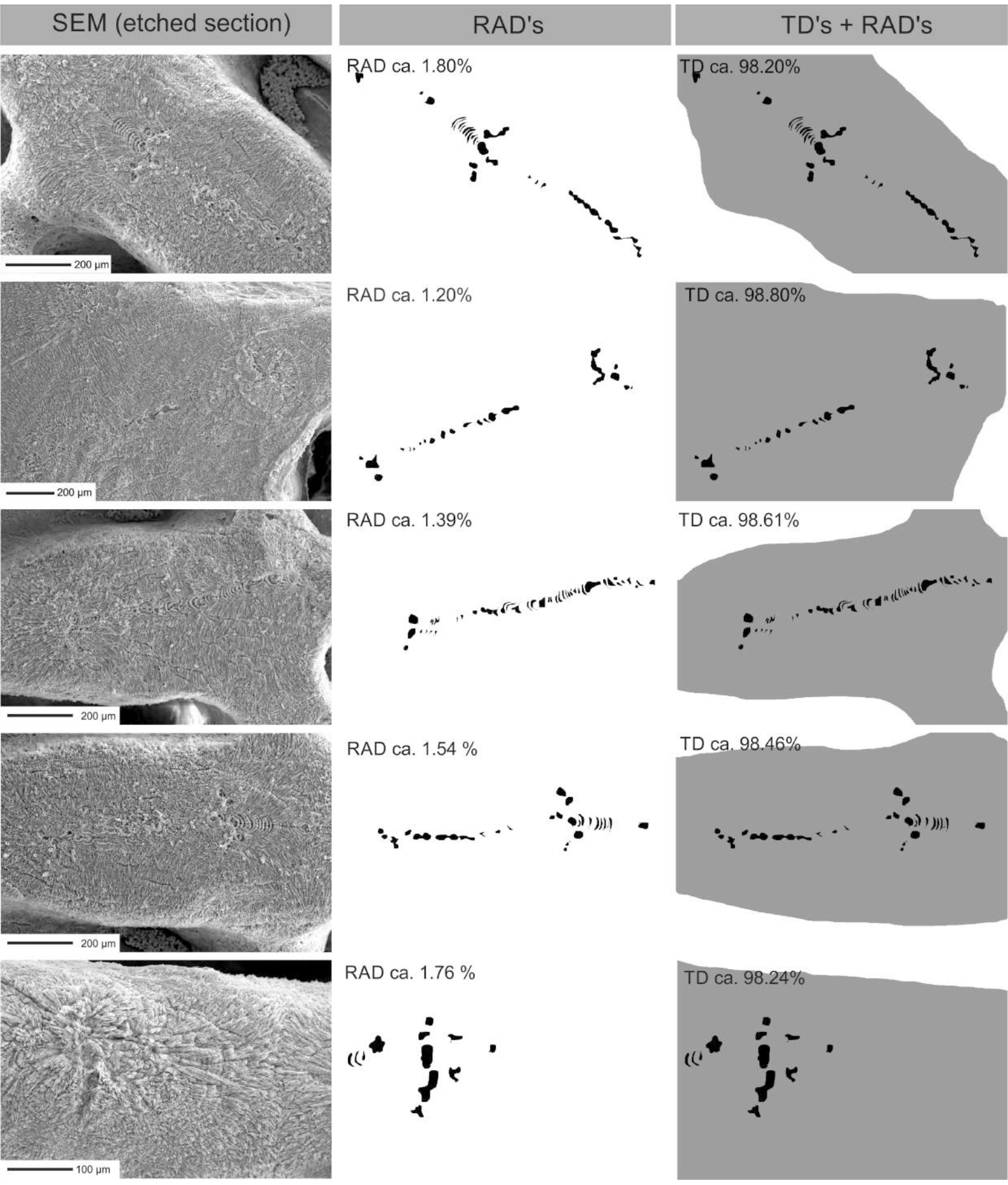
SEM (etched section)
RAD's
TD's + RAD's
RAD ca. 1.80%
TD ca. 98.20%
200 µm
RAD ca. 1.20%
TD ca. 98.80%
200 µm
RAD ca. 1.39%
TD ca. 98.61%
200 µm
RAD ca. 1.54 %
TD ca. 98.46%
200 µm
RAD ca. 1.76 %
TD ca. 98.24%
100 µm

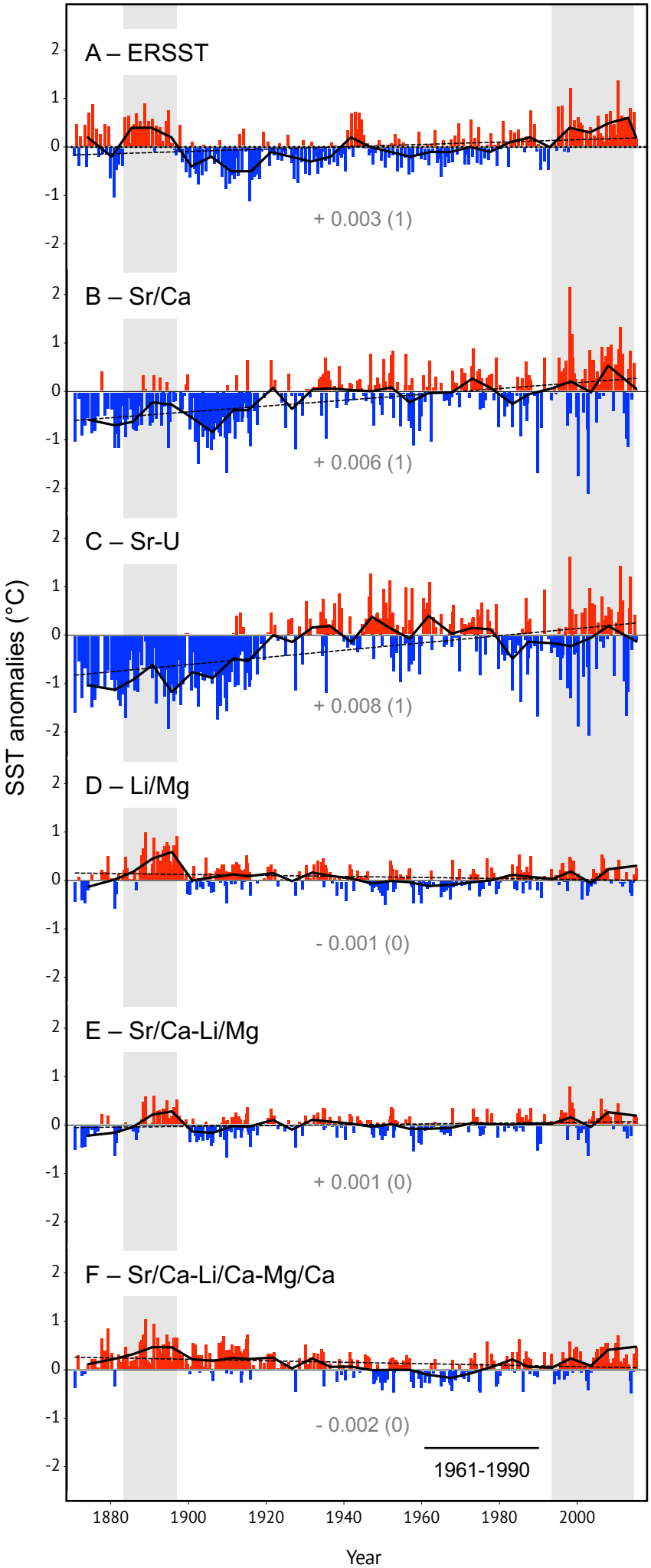
A – ERSST
+ 0.003 (1)
B – Sr/Ca
+ 0.006 (1)
C – Sr-U
+ 0.008 (1)
D – Li/Mg
- 0.001 (0)
E – Sr/Ca-Li/Mg
+ 0.001 (0)
F – Sr/Ca-Li/Ca-Mg/Ca
- 0.002 (0)
1961-1990
SST anomalies (°C)
Year
1880
1900
1920
1940
1960
1980
2000